Design, Synthesis and Pharmacological Evaluation of Non-Steroidal Tricyclic Ligands as Modulators of $GABA_A$ Receptors

Yue Xu [†, #, ‡], *Martin Mortensen* [§, ‡], *Seth Liebowitz* [§], *Nicoline N. Jensen* [†], *Yongsong Tian* [†], *Francesco Bavo* [†], *Thomas Seidel* [¥], *Trevor G. Smart* [§, *], *Bente Frølund* [†, *]

[†] Department of Drug Design and Pharmacology, Faculty of Health and Medical Sciences, University of Copenhagen, Universitetsparken 2, DK-2100 Copenhagen, Denmark.

[#] State Key Laboratory of Natural and Biomimetic Drugs, School of Pharmaceutical Sciences, Peking University, Beijing, 100191, China.

[§] Department of Neuroscience, Physiology & Pharmacology, University College London, Gower Street, London WC1E 6BT, UK.

[¥] Department of Pharmaceutical Sciences, Division of Pharmaceutical Chemistry, University of Vienna,1090 Vienna, Austria.

[‡] Authors contributed equally (Yue Xu and Martin Mortensen)

[*] Corresponding Authors - Bente Frølund (bfr@sund.ku.dk) and Trevor G. Smart (t.smart@ucl.ac.uk).

KEYWORDS: γ-Aminobutyric Acid Type A Receptors ($GABA_A$Rs), Neuroactive steroids (NASs), Shape similarity, Structural decomposition, Whole-cell patch clamp.

ABSTRACT $GABA_A$ receptors ($GABA_A$Rs) are the major elements of inhibitory neurotransmission in the central nervous system (CNS). They are established targets for regulation by endogenous brain neuroactive steroids (NASs) such as pregnanolone and pregnenolone sulfate (PS). Indeed, derivatives of pregnanolone have been developed to treat disorders including postpartum depression and major depressive disorder. However, the complexity of de novo synthesis of NAS derivatives has hindered attempts to circumvent the principal limitations of using endogenous NASs, including target selectivity, overly fast metabolism, and limited oral bioavailability. In this study, we designed a series of tricyclic compounds, inspired by the structures of pregnanolone and pregnenolone sulfate, to explore novel non-steroidal alternatives. Using patch clamp electrophysiology, we demonstrate that these compounds exhibit either positive or negative allosteric modulation of $GABA_A$Rs. Specifically, we discover a new positive allosteric modulator (PAM), and a series of tricyclic sulfate-based negative allosteric modulators (NAMs) that are all active at micromolar level. This research has significantly broadened the chemical diversity of ligands targeting $GABA_A$Rs. It also creates an opportunity for discovering more efficacious allosteric modulators while avoiding the complexity of de novo NAS synthesis and limitations associated with their derivatization.

Introduction

γ-Aminobutyric Acid Type A Receptors ($GABA_A$Rs) play a pivotal role for inhibitory neurotransmission within the central nervous system (CNS).[1] As pentameric ligand-gated ion channels, these receptors mediate fast synaptic and persistent tonic inhibition following activation by the neurotransmitter γ-aminobutyric acid (GABA). Together, they regulate neuronal excitability and thus play an essential role in neural communication and homeostasis. Consequently, dysregulation of $GABA_A$Rs has been implicated in numerous neurological disorders, emphasizing their importance as drug targets for the treatment of various CNS-related diseases.[2]

Endogenous brain neuroactive steroids (NASs) function as either positive or negative allosteric modulators (PAMs, NAMs) of $GABA_A$Rs to regulate their activity.[3] The identification of physiologically-important binding sites for NASs on $GABA_A$Rs remains an evolving subject.[4-7] Diverse methodologies, including site-directed mutagenesis and homology modelling, photolabeling, X-ray crystallography and cryo-EM, have all contributed to the identification of three distinct potentiating steroid binding sites on the heteromeric $GABA_A$Rs with a strong consensus for the interfacial β-α subunit site.[4, 6, 8] Conversely, recent studies have proposed another mechanism for inhibition by NASs, favoring a pore block model over the alternative receptor-lipid interface interaction.[4, 7] This highlights the complexity and evolving understanding of NASs interactions with $GABA_A$Rs. Allopregnanolone and pregnanolone are equipotent PAMs potentiating the receptor's response to GABA, underlying its importance in CNS physiology and potential for therapeutic applications.[5, 9] (Figure 1). Indeed, brexanolone (allopregnanolone) is FDA-approved for moderate-to-severe postpartum depression, but requires intravenous administration.[10, 11] Recent developments in synthetic analogs have produced Zuranolone (SAGE-217) that is orally active, significantly enhancing patient compliance and expanding its application to both postpartum and major depressive disorders.[12-14] Conversely, endogenous 3β-OH and sulfated steroids are capable of inhibiting GABA-elicited currents, such as epi-allopregnanolone, pregnenolone sulfate (PS) and dehydroepiandrosterone sulfate (DHEAS).[15, 16] Ganaxolone, an investigational $GABA_A$Rs-modulating steroid, is an improved drug for treatment of seizures associated with cyclin-dependent kinase-like 5 (CDKL5) deficiency disorder.[17] Despite their physiological and potential therapeutic relevance, the use of steroidal modulators is constrained by limitations including poor pharmacokinetic properties and potential off-target effects.[18] Furthermore, the synthetic complexity inherent to steroidal frameworks further restricts their derivatization, presenting a significant chemical bottleneck in the pursuit of optimizing their pharmacological profiles.

To circumvent these issues, we designed and synthesized a series of tricyclic non-steroidal allosteric modulators, which transcend the synthetic and derivatization limitations imposed by steroidal scaffolds. This approach permits the identification of potentially-active non-steroidal ligands. Such an approach broadens chemical space and offers the potential for improved drug property profiles, including enhanced target selectivity,[19] optimized pharmacokinetic profiles,[20] whilst minimising off-target interactions with, for example, the NMDA receptor,[21]. Collectively this will enhance the therapeutic potential of $GABA_A$R modulators.

In this study, we designed a series of non-steroidal ligands based on a tricyclic ring system that targets $GABA_A$Rs by exploring both their shape similarity to the endogenous steroidal modulators, pregnanolone and PS, and their ability to bind to NAS binding sites. This led to the identification of a non-steroidal compound acting as a PAM, identified through the juxtaposition of steroidal and non-steroidal shape similarity with pregnanolone; and, in a complementary approach, a series of compounds were synthesized employing a structural deconstruction approach for PS, with the majority of these non-steroidal derivatives displaying NAM activity. This dual-faceted exploration not only augments the ligand pool for GABA$_A$R modulation but also extends our understanding of the structural and functional nuances operating at the NAS binding sites.

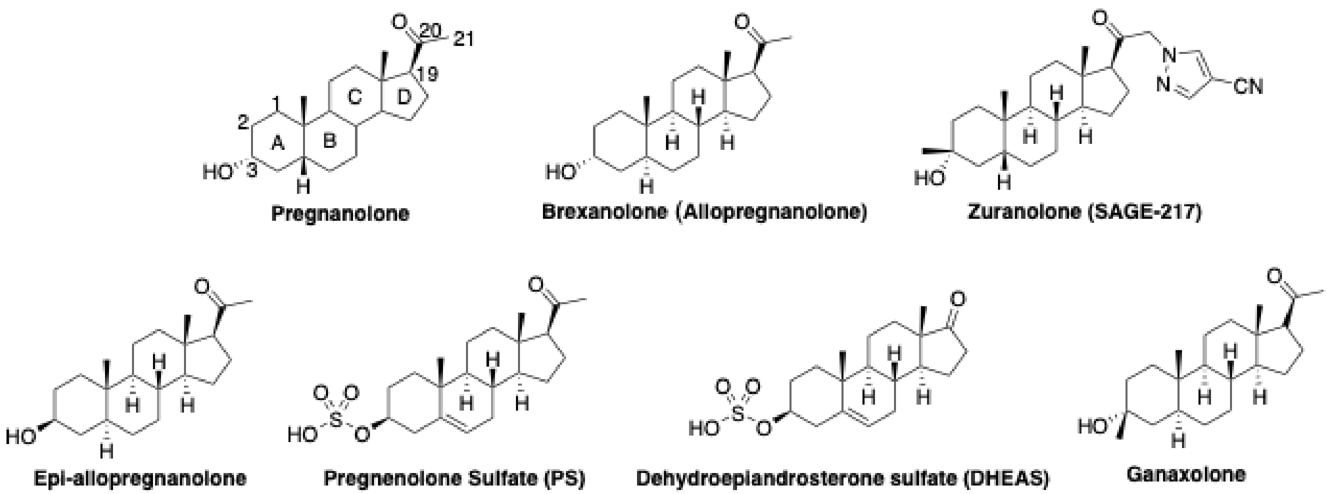

Figure 1. Chemical structures of representative natural and synthetic neuroactive steroids (NASs).

Results

Design of a non-steroidal PAM by shape similarity analysis. Using our knowledge of the pregnanolone interfacial $\beta^+\alpha^-$ subunit binding site in GABA$_A$Rs, we proposed that a collection of synthetic, protein-binding, non-steroidal ligands could be docked at the NAS-binding site to serve as a ligand library, facilitating scaffold hopping from pregnanolone to potentially functional non-steroidal structures (Scheme 1). To assemble such a collection of non-steroidal ligands that may mimic pregnanolone at GABA$_A$Rs, we first compiled a group of reference steroids that bind to different proteins (eg, estradiol bound to the estrogen receptor, dihydrotestosterone bound to the androgen receptor, and progesterone bound to the progesterone and also mineralocorticoid receptors; see Methods). We then selected a series of non-steroidal molecules based on the following criteria: 1. Both the reference steroids and non-steroidal ligands interacting with proteins must be retrievable from the RCSB Protein Data Bank. 2. The reference steroids must structurally resemble pregnanolone, characterized by the presence of a H-bond donor or acceptor at each end of the molecule in rings A and D, respectively. 3. Only those non-steroidal ligands that predominantly overlap with the aliphatic rings of the reference steroids, as determined by structural superimposition, were selected.

By adopting these criteria, a collection of 34 non-steroidal ligands were identified for further investigation. For the reference steroids, the predominant determinants of binding affinity are lipophilic contacts with the steroid's aliphatic ring core. The binding energy contributed by H-bonding polar groups in rings A and D is relatively low, but it is imperative to note that the configuration of the C3 hydroxyl group in ring A determines the allosteric modulatory nature of NASs.[5] Given the combined significance of the aliphatic ring structures and H-bonding in promoting pregnanolone efficacy, it became evident that a 3D shape similarity-based technique would be best-suited for performing pregnanolone scaffold hopping. This methodology capitalizes on molecular alignment facilitated through OpenEye's ROCS (Rapid Overlay of Chemical Structures) software,[22] utilizing an optimization strategy centered on maximizing the molecular volume overlap. The query molecule we used to scrutinize our library of non-steroidal ligands was pregnanolone (PDB 5O8F) without further modification.[5] Given the limited structural diversity of pregnanolone-based ligands at its interfacial binding site, using the ROC (receiver operating characteristic) curve or ligand enrichment for analyzing the query molecule was deemed inappropriate. We used OpenEye's conformational generator, OMEGA, to generate conformers of all 34 non-steroidal ligands,[23] while ROCS served as a tool for conducting shape similarity analyses. For this analytical process, the 34 ligands were ranked according to shape Tanimoto, resulting in 12 non-steroidal molecules exceeding 0.7. This threshold is commonly used for identifying molecules with significant similarity to the query molecule. Therefore, a relatively high proportion of non-steroidal structures resembled the shape of pregnanolone (Table S1). One such ligand (PDB 5KRM) exhibited the highest Shape-Tanimoto score of 0.814. This pregnanolone-based compound was designated as our lead structure due to its significant overlap in both shape and projected electrostatic interactions (Figure 2A). To more accurately mimic pregnanolone, the non-steroidal ligand was converted into compound **3b** by removing two fluorine atoms and incorporating a single acetyl group into the phenyl ring. (Figure 2B)

Scheme 1. Workflow for the identification of non-steroidal ligand resembling pregnanolone.

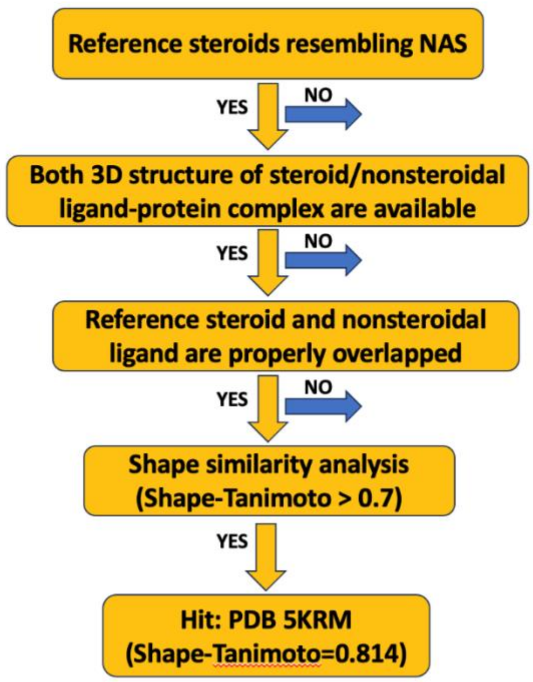

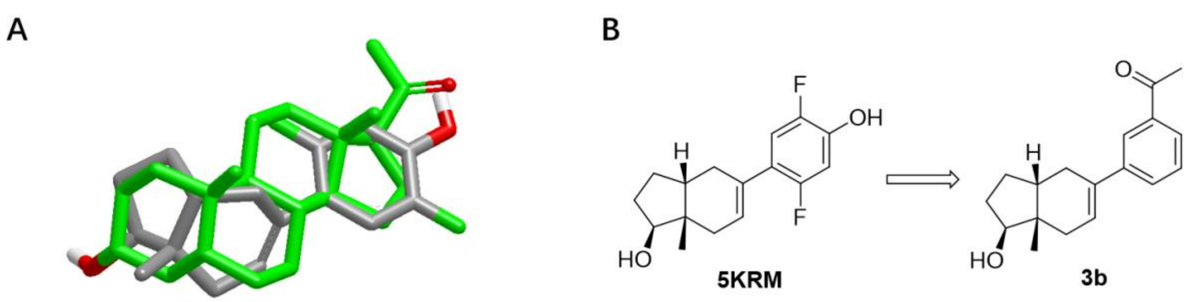

Figure 2. The design of target compound **3b** that overlays pregnanolone. A: overlaid poses of pregnanolone (green) and the 5KRM ligand (grey) bound to the estrogen receptor (ER; PDB: 5KRM). B: structures of the ligand (PDB: 5KRM) and its non-fluoro, acetyl derivative **3b**.

Design of non-steroidal NAMs by deconstruction of an inhibitory NAS. The positioning of the inhibitory NAS, PS, at the interface between the $GABA_AR$ and the lipid bilayer as suggested in the chimeric GLIC-$GABA_AR\alpha1^{G258V}$ X-ray crystal structure infers that docking might not be the optimal approach for investigating the binding site.[4] In addition, according to a cryo-EM study, PS can bind within the ion channel of recombinant $GABA_A$ receptor, resulting in a different set of PS-protein interactions.[7] In this study, various orientations of inhibitory NASs were sampled by cryo-EM and molecular dynamics (MD) simulations, highlighting the inherent variability and lack of shape complementarity in the location of the binding site.[7] Consequently, we decided to take an alternative approach by initiating a systematic investigation of the PS ring system. This strategy involved simplifying the steroidal scaffold to various tricyclic systems while maintaining the overall original molecular configuration of PS, with the aim of finding the minimally-active scaffold for PS (Scheme 2). In addition, one of the tricyclic rings was transformed into an aromatic ring, both to explore potential pharmacophore elements at the PS binding site and to simplify the chemistry required for subsequent derivatization. Previous SAR studies and cryo-EM structures of inhibitory NASs highlighted several features relevant for activity. (1) The type and configuration of the substituent at C3 plays a pivotal role in the modulatory effect of NASs and distinguishes between a NAS PAM and NAM.[24] (2) Either a hydroxyl or sulfate substituent at the C3 position supports inhibition by the NASs, with the sulfate being more potent.[25] (3) Given the cryo-EM structure of the $GABA_AR$ bound with PS, and considering that DHEAS is a $GABA_AR$ NAM, the C20 H-bond acceptor in PS might not be essential for receptor modulation.[4] Accordingly, we designed a series of synthetically tractable compounds with a tricyclic system containing either a C3-sulfate or -hydroxyl group (Scheme 2). The core structure of compound **3** was employed as the scaffold template for derivatives featuring the ABD tricyclic ring system. In the structural design of compound **4**, we incorporated a bromine atom onto the phenyl ring. This strategy was guided by our prior work indicating that the C-21 position in the PS could accommodate larger groups.[26] By introducing a bromine atom we could probe the spatial allowance at this end of the molecule. Furthermore, this substitution will facilitate future derivatization through coupling reactions. These compounds align well with PS in terms of their respective ring core and the chemical features of the substituent group resident at C3 (Figure 3).

Scheme 2. Structural decomposition of pregnenolone sulfate. *[a]*

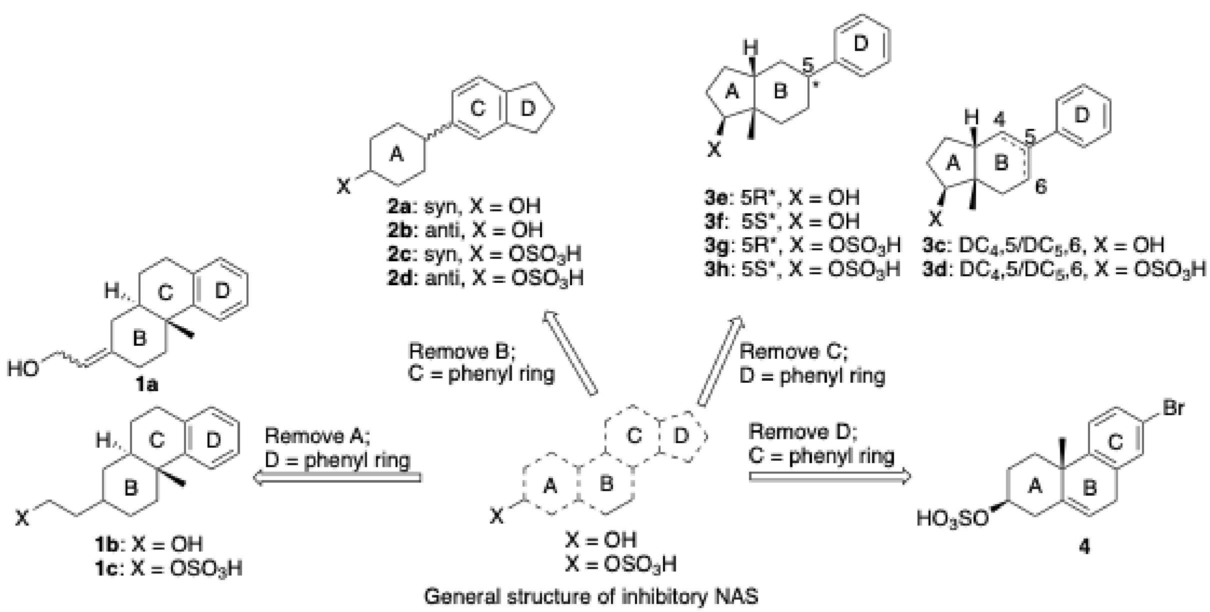

*[a]*When the stereochemistry at one stereocenter remains unknown, an asterisk (*) is added to indicate that the assignment could be opposite.

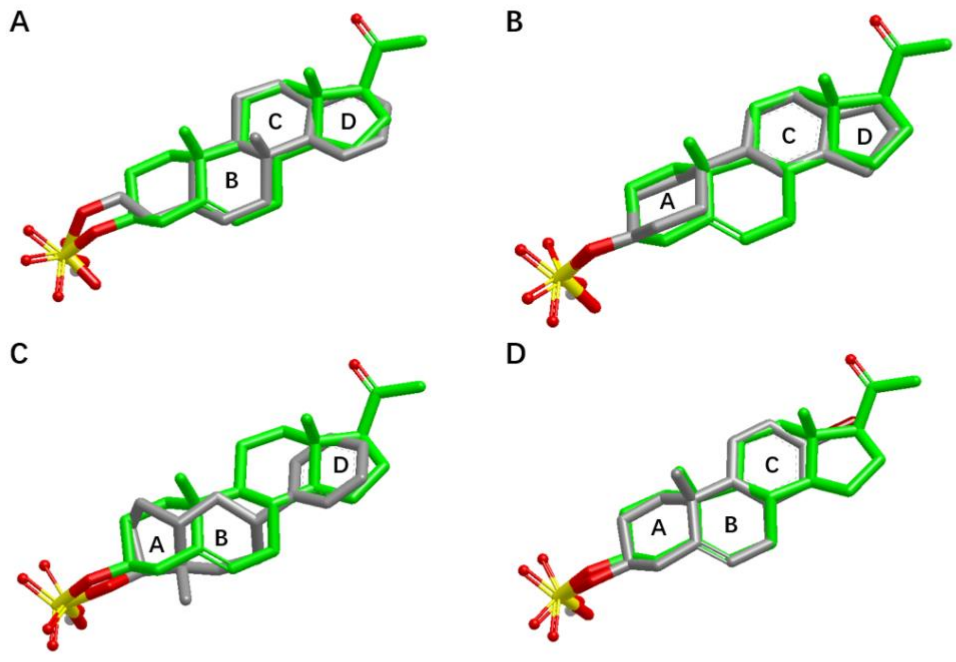

Figure 3. Structural overlap analysis between representative non-steroidal sulfate ligands (grey) and PS (green). Note the significant alignment of PS rings along with well-matched positioning of the C3 sulfate group using Openeye ROCS software. (A) compound **1c** with a BCD ring system (B) compound **2d** with a ACD ring system, (C) compound **3h** with the ABD ring system, and (D) compound **4** with the ABC ring system.

Synthesis of Target Compounds.

Analogs with BCD system. In the proposed synthetic route, we presumed that the desired compounds bearing a BCD ring system can be synthesized from the tricyclic keto intermediate **9** through a Horner–Wadsworth–Emmons (HWE) reaction,[27] as delineated in Scheme 4. The construction of intermediate **9** was initiated by the treatment of 1-methyl-3,4-dihydronaphthalen-2(1H)-one with (S)-α-methylbenzylamine, followed by the azeotropic removal of water and addition of methyl vinyl ketone (MVK), predominantly yielding the bridged ketol **5**, as previously reported by Morgen *et al*.[28] (Scheme

3). Further reaction of **5** with PTSA in toluene furnished the key intermediate **6**. The protection of the carbonyl group, catalytic hydrogenation and subsequent deprotection, afforded intermediate **9**, which is characterized by a favorable selectivity for forming trans-fused rings in toluene.[29] The requisite side chain was introduced in intermediate **9** utilizing the HWE reaction, yielding an isomeric mixture of (*E*/*Z*)-**10**, that was used without additional purification (Scheme 4). Initial attempts to synthesize **1b** involved the reduction of ester (*E*/*Z*)-**10** to (*E/Z*)-**1a**, followed by catalytic hydrogenation using Pd/C in methanol at ambient temperature. This approach, however, was unsuccessful in hydrogenating (*E*/*Z*)-**1a** to **1b**, leading instead to the unintended elimination of the hydroxyl group. Therefore, hydrogenation of (*E/Z*)-**10** to **11** was performed prior to ester reduction, which successfully yielded **1b** as a mixture of diastereomers. This mixture was then converted to the sulfated derivative as a mixture of diastereoisomers, **1c**. As compound (*Z*)-**1a** exhibited markedly higher shape similarity to PS compared to compound (*E*)-**1a**, so the presumed (*Z*)-**1a** was isolated using preparative high-performance liquid chromatography (prep-HPLC) and its structure was characterized through Rotating-frame Overhauser Effect Spectroscopy (ROESY). (Figure S1). However, Z configuration could not be conclusively determined.

Scheme 3. Synthesis of intermediate 9 for generating compounds with BCD rings.[a]

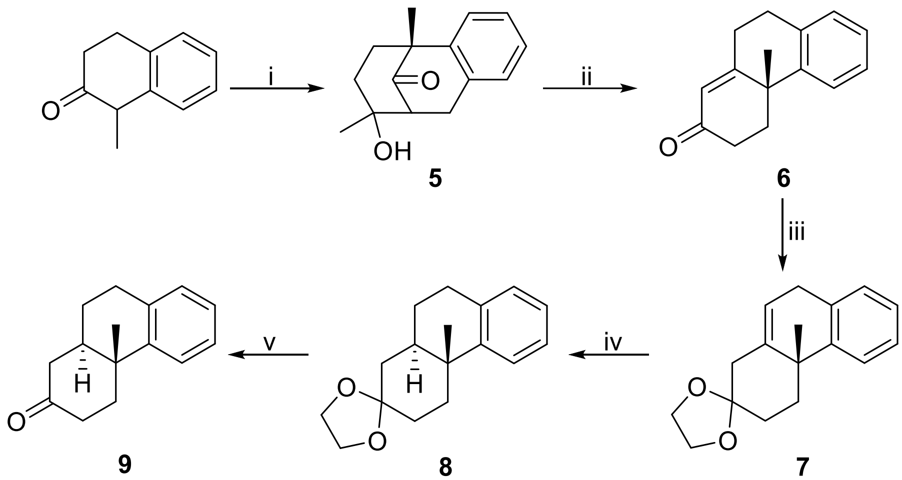

[a]Reagents and conditions: (i) (a) (*S*)-α-methylbenzylamine, toluene, reflux.; (b) MVK, THF; (ii) PTSA, toluene, reflux; (iii) ethylene glycol, PTSA, benzene, reflux; (iv) $Pd(OH)_2$, H_2, 50 psi, toluene, 50 °C. (v) 2M HCl, ethanol, rt.

Scheme 4. Synthesis of compound 1a – 1c incorporating a BCD ring system.[a]

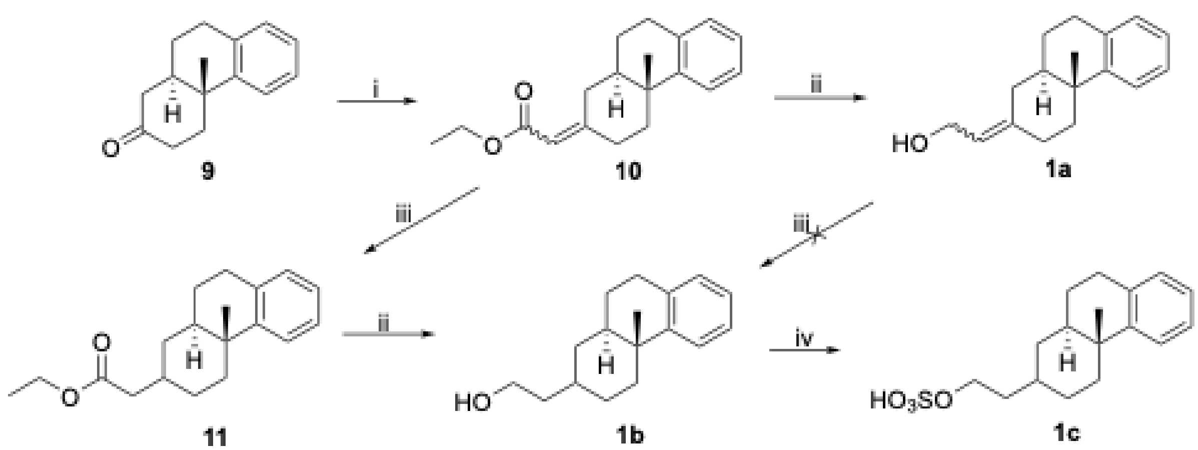

[a]Reagents and conditions: (i) triethyl phosphonoacetate, NaH, DMF, rt; (ii) DIBAL-H, THF, 0 °C – 40 °C; (iii) Pd/C, H_2, 1 atm, MeOH, rt; (iv) pyridine sulfur trioxide, pyridine, chloroform, rt.

Analogs with ACD system. To prepare compounds with an ACD ring system, bromine–lithium exchange was anticipated to enable the fusion of A and CD rings (Scheme 5). Therefore, 4-((tert-butyldimethylsilyl)oxy)cyclohexan-1-one was reacted with (2,3-dihydro-1H-inden-5-yl)lithium (prepared *in-situ*), providing **12**, that was then dehydrated and hydrogenated, to the diastereomers **2a** and **2b**, separated by silica-gel chromatography and characterized by ROESY (Figure S2). The two diastereomers were subsequently converted to sulfated derivatives **2c** and **2d**.

Scheme 5. Synthesis of compounds 2a–2d with ACD rings system[a]

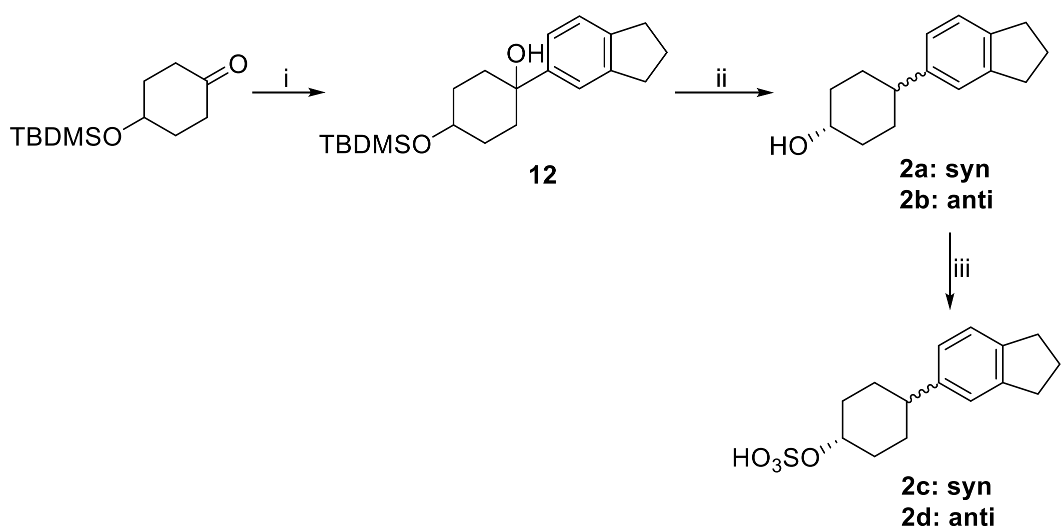

[a]Reagents and conditions: (i) 5-bromo-2,3-dihydro-1H-indene, *n*-BuLi, THF, -78 °C; (ii) 1M HCl, ethanol; Pd/C, H_2, 1 atm, rt; (iii) pyridine sulfur trioxide, pyridine, chloroform, rt.

Analogs with ABD system. The skeleton of **3b**, intended as a non-steroidal ligand analogous to pregnanolone, was also utilized as the ABD ring system in the PS deconstruction strategy. The synthesis was initiated with the assembly of the *cis*-fused AB rings. The triketone **13** was obtained by reacting MVK and 2-methylcyclopentane-1,3-dione (Scheme 6). Subsequently, the enantiomerically pure diketone **14** was synthesized via L-proline catalyzed asymmetric Robinson annulation, following the

Hajos-Parrish protocol.[30] Acidic treatment of hydroxyl diketone **14** allowed rapid elimination, yielding unsaturated diketone **15**.[31] Reduction of the diketone **15** to **16** was achieved in a chemo- and stereo-selective manner using ethanolic $NaBH_4$, as reported.[31] Selective hydrogenation of **16** in liquid ammonia with lithium yielded **17**, characterized by *cis*-fused AB rings (Figure S3), that was later protected to intermediate **18**. Despite the absence of a comprehensive mechanistic study for the selective hydrogenation, Zeng *et al.* proposed an intramolecular proton transfer from the hydroxyl group to the radical anion, leading to the major *cis*-fused rings product.[32] Lithiated 2-(3-bromophenyl)-2-methyl-1,3-dioxolane or phenyl bromide were reacted with the TBDMS protected intermediate **18**, producing epimeric tertiary alcohols **19a** or **19b**, respectively (Scheme 7). Subsequent acidic treatment facilitated hydroxyl group elimination and TBDMS deprotection, leading to a regioisomeric mixture of **3a/b** or **3c**, respectively. Since **3a/b** later showed interesting pharmacology, the regioisomers were resolved using chiral preparative HPLC (Figure S4) into **3a** and **3b**, which were characterized by Correlation Spectroscopy (COSY) and ^{1}H NMR. (Figure S5, S6) However, the separation of **3c** regioisomers was unsuccessful, and they were therefore tested as mixture of **3c**$_{\Delta 5,6}$: **3c**$_{\Delta 4,5}$ in a ratio of 11 to 19, characterized by COSY. (Figure S7). The anticipated NAM **3d** was synthesized by sulfonation of **3c** (Scheme 8). Additionally, hydrogenation of **3c** yielded the diastereoisomer mixtures **3e**/**3f**, which was further separated using HPLC and attempted characterized by ROESY (Figure S8) but no conclusive assignment was obtained. Finally, each diastereoisomer was sulfonated to **3g**/**3h**.

Scheme 6. Synthesis of compound 18 for deriving compounds with an ABD ring system[a]

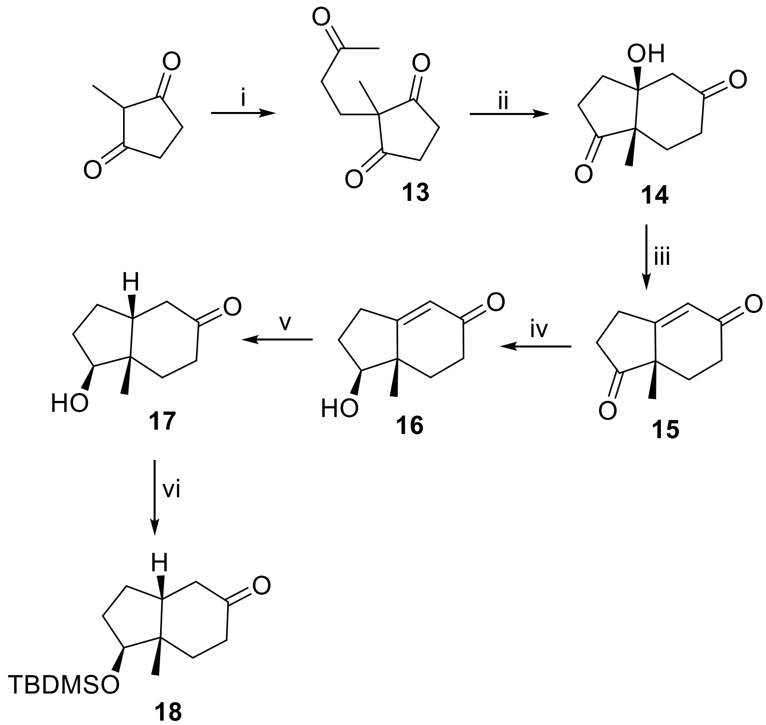

[a]Reagents and conditions: (i) MVK, AcOH, H_2O, 75 °C; (ii) L-proline, DMF, rt., (iii) H_2SO_4, DMF, 95 °C; (iv) $NaBH_4$, ethanol, -18 °C; (v) Li, liquid NH_3, -78 °C; (vi) TBDMSCl, imidazole, DMF, rt.

Scheme 7. Synthesis of compound 3a–3c with the ABD ring system[a]

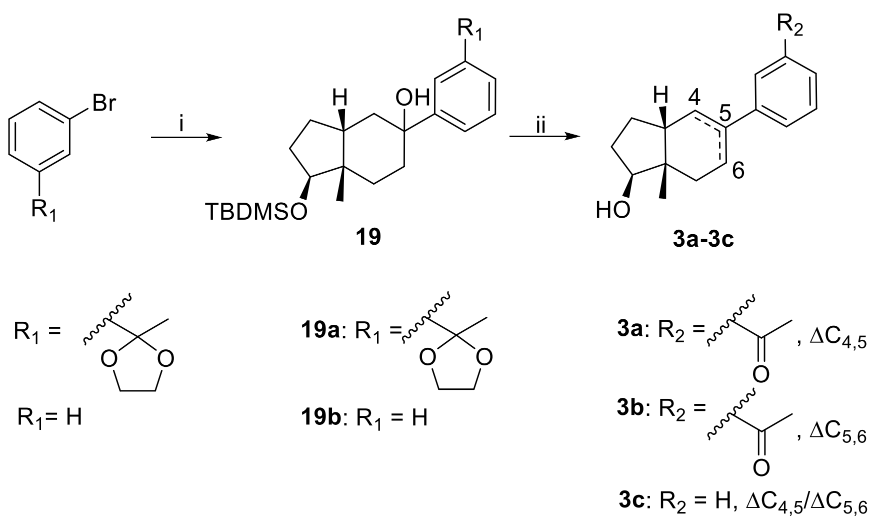

[a]Reagents and conditions: (i) *n*-BuLi, THF, **18**, -78 °C; (ii) 1M HCl, ethanol, rt.

Scheme 8. Synthesis of compound 3d–3h with the ABD ring system[a]

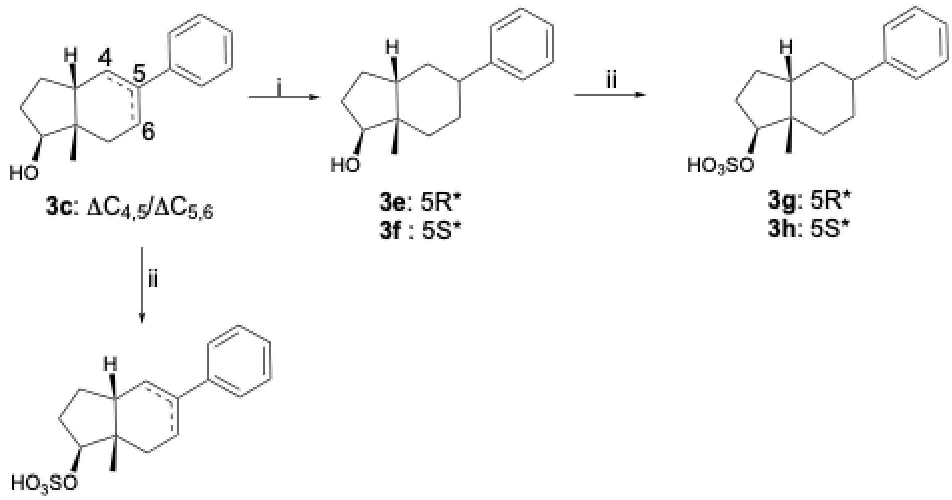

3c: $\Delta C_{4,5}/\Delta C_{5,6}$ **3e**: 5R* **3f** : 5S* **3g**: 5R* **3h**: 5S* **3d**: $\Delta C_{4,5}/\Delta C_{5,6}$

[a]Reagents and conditions: (i) Pd/C, methanol, H_2, rt; (ii) pyridine sulfur trioxide, pyridine, chloroform, rt. When the stereochemistry at one stereocenter remains unknown, an asterisk (*) is added to indicate that the assignment could be opposite.

Analogs with ABC system. For mirroring the chirality of AB rings in PS, the synthesis of the non-steroidal compound featuring an ABC ring system commenced with the treatment of (*R*)-α-methylbenzylamine with 6-bromo-1-methyl-3,4-dihydronaphthalen-2(1H)-one to initiate enantioselective Michael alkylation utilizing MVK, yielding the intermediate **20** (Scheme 9), as delineated by Gan et al.[33] Acidic treatment converted **20** to key tricyclic intermediate **21**, establishing the conformation of the AB rings. Intermediate **21** was first converted to its corresponding dienol acetate derivative and then reduced with $NaBH_4$ to **22**. Concluding the synthesis, standard sulfonation efficiently transformed compound **22** to **4**, yielding the anticipated PS-like NAM.

Scheme 9. Synthesis of compound 4 with an ABC ring system[a]

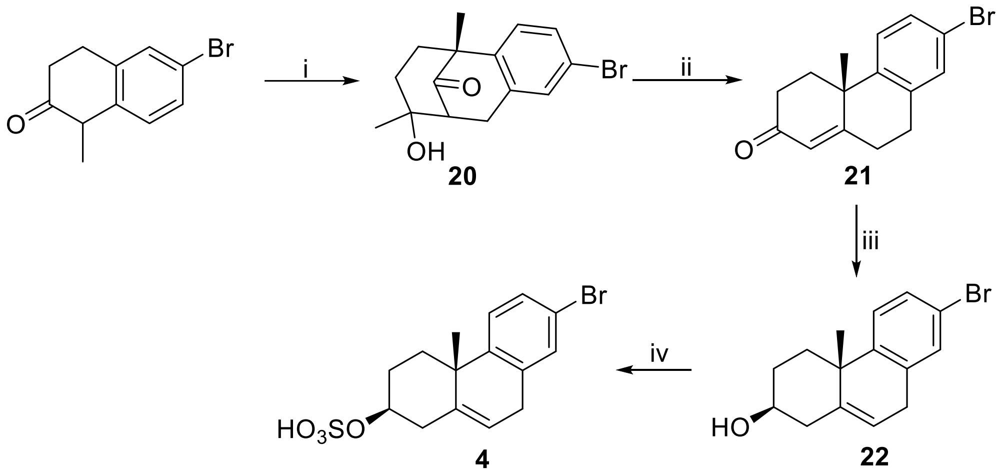

[a]Reagents and conditions: (i) (a) (*R*)-α-methylbenzylamine, toluene, reflux; (b) MVK, THF; (ii) PTSA, toluene, reflux; (iii) Ac_2O, EtOAc, 70% $HClO_4$, rt.; $NaBH_4$, EtOH, 0 °C; (iv) pyridine sulfur trioxide, pyridine, chloroform, rt.

Pharmacological Characterization on recombinant GABA$_A$Rs. This new set of non-steroidal compounds was based on the molecular shapes of two NAS ligands with very different functional effects on GABA$_A$Rs; one being a PAM, pregnanolone, and the other a NAM, pregnenolone sulphate (PS). However, as these non-steroidal neurosteroid-like compounds are quite different structurally from their reference NAS, we investigated their functional effects for comparison with their expected profiles. This involved testing all the novel compounds for direct activation, as well as PAM and NAM effects, using whole-cell patch clamp recording of HEK cells expressing recombinant $\alpha_1\beta_3\gamma_2$ GABA$_A$Rs.

For assessing direct activation by the non-steroidal derivatives at GABA$_A$Rs, we applied the highest soluble concentration for each compound (all 100 μM). When setting an arbitrary level of 5% of the maximal GABA current evoked by 1 mM GABA, the compounds which displayed direct activation were, **2a–c**, **3a/b**, **3c**, **3e–g** and **4**. The largest effect was displayed by **3f** (43 ± 5 % of GABA$_{Max}$; Figure 4A, B), where the mean direct activation effect by **3f** was significantly greater than all the other compounds (all $p < 0.0001$; Figure 4B, blue asterisks). Interestingly, of the four other compounds which showed the highest direct receptor activation (**2a**, red; **2b**, green; **3c**, purple, and **3f**, blue), none carried the sulfate group. Only these four compounds showed significant differences from the other non-steroidal compounds as shown in Figure 4B (all other Tukey's post-hoc comparisons between compounds were not significant; not shown).

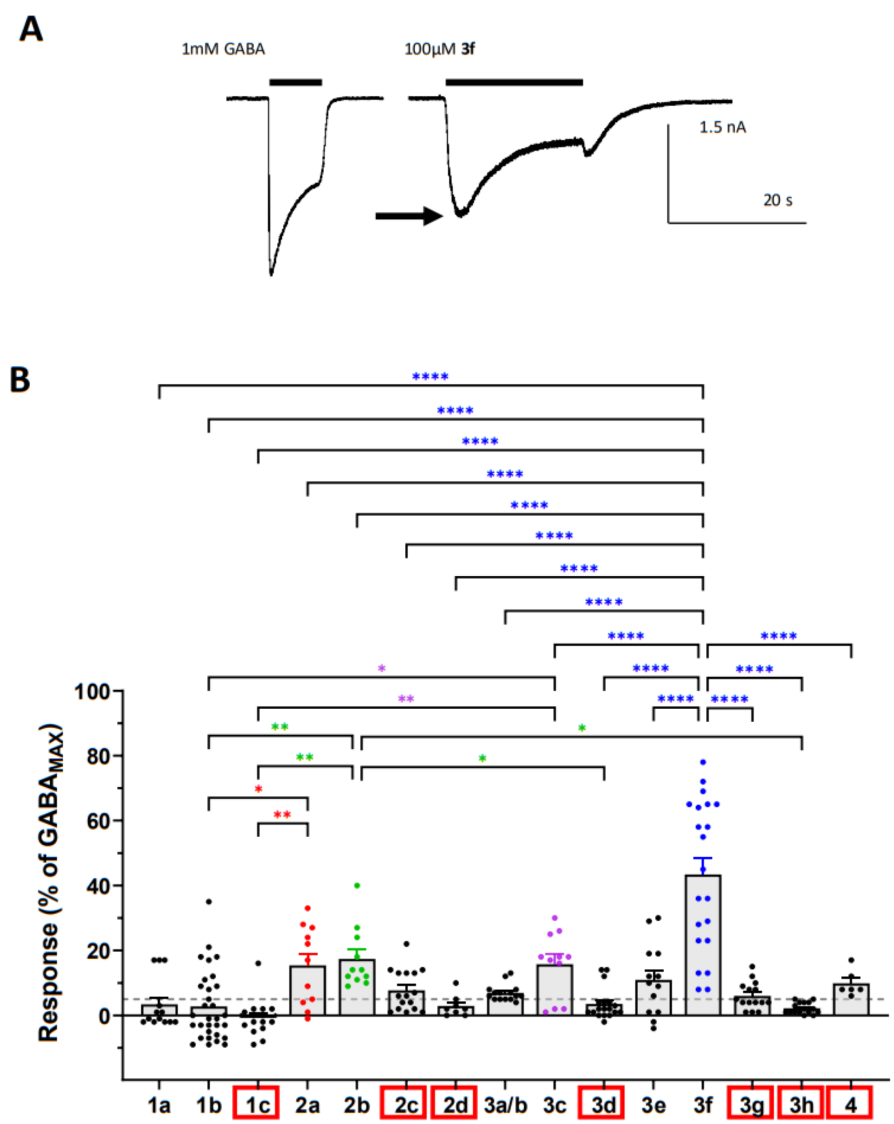

Figure 4. Direct activation of $GABA_ARs$ by novel non-steroidal compounds. Whole-cell voltage-clamp electrophysiological assessment of direct activation of compounds on $\alpha_1\beta_3\gamma_2$ $GABA_ARs$ transiently expressed in HEK cells. All drugs were applied at their maximum solubility of 100 μM. (A) Representative example of current responses to GABA and **3f**. The response (% of $GABA_{Max}$) was calculated from the peak (arrow) of any direct drug activation compared with the maximum current obtained with 1 mM GABA. (B) Histogram showing direct activation levels for all compounds tested. Red boxes indicate sulfated compounds. An arbitrary 5% threshold limit for direct activation is shown as a stippled line. Each bars show the mean ± SEM, with individual values shown as dots. All compounds were compared in a one-way ANOVA ($F_{14, 205} = 21$; $p < 0.0001$), and subsequently in a Tukey's multiple comparisons test. All statistically significant comparisons are shown on the histogram (*: $p < 0.05$; **: $p < 0.01$; ****: $p < 0.0001$).

To investigate the inhibitory potential of the non-steroidal compound series, we studied the potential for all compounds to inhibit a whole-cell current response induced by 70 μM GABA, which equates to EC_{80-90} on recombinant $\alpha_1\beta_3\gamma_2$ $GABA_ARs$. We have previously found that inhibitory effects are more readily detected when using agonist concentrations of EC_{80-90}, rather than at over-saturated concentrations ($\geq EC_{100}$).

Concentration-response studies were performed for all compounds up to the highest concentration of 100 μM. Both the initial inhibition of the peak, as well as the inhibition level at steady-state was assessed, and to ensure binding by the compounds before GABA activation we pre-applied these compounds prior to co-application with GABA (Figure 5A). The reason for also measuring the steady-state level was that inhibitory NASs, like PS, previously have been shown to affect the extent of desensitization (observed at the steady-state level) much more readily than receptor activation (observed by peak current depression).[34]

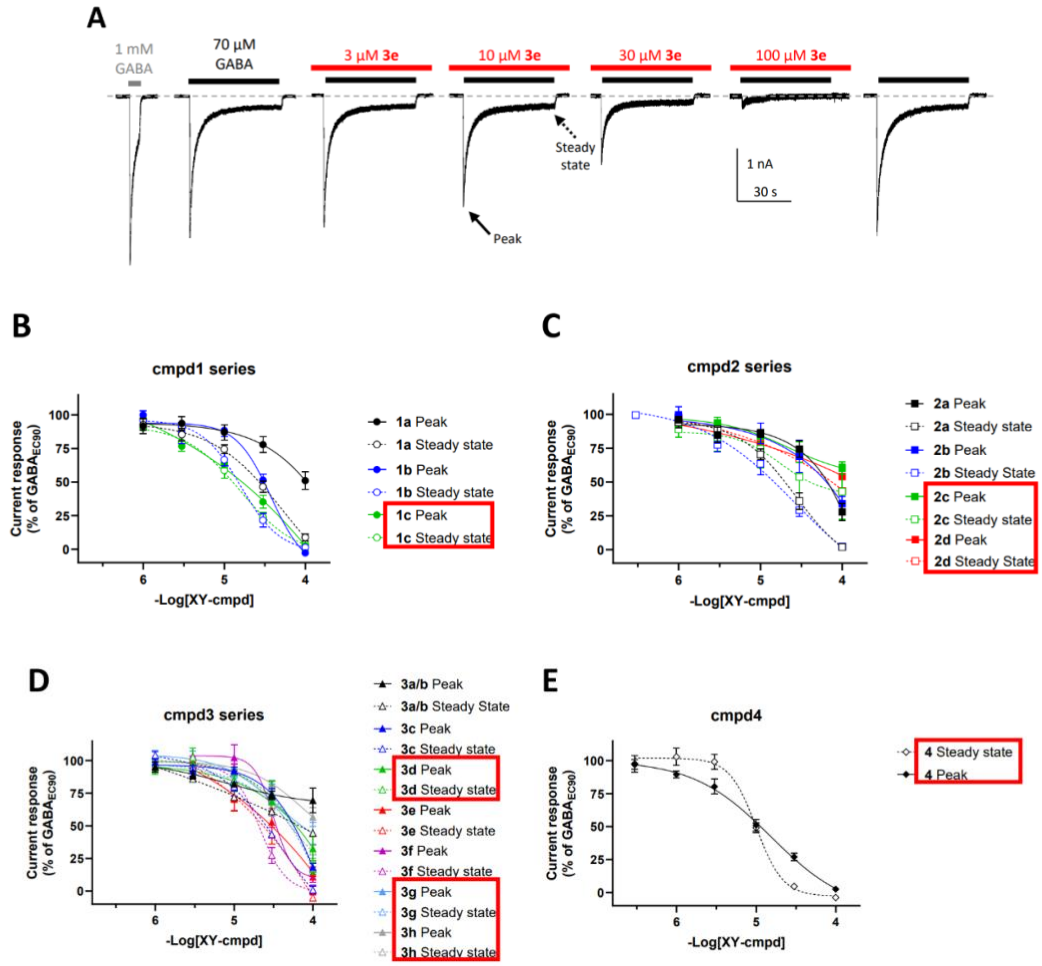

Figure 5. Inhibitory effects of non-steroidal compounds on GABA$_A$Rs. Concentration-response evaluation of the inhibitory effect of compound series **1** – **4** on $\alpha_1\beta_3\gamma_2$ GABA$_A$Rs. Red boxes indicate sulfated compounds. (A) Representative current responses to a maximum GABA concentration (1 mM), and to 70 µM GABA (~ EC$_{80}$), with or without increasing concentrations of pre-applied **3e**. Measurements were taken from the peak (solid arrow) and from when the current has reached a fully inhibited/desensitised steady state level (stippled arrow). Concentration-inhibition curves for peak and steady-state responses for compound series **1** – **4** are shown in panels B, C, D and E, respectively. Fitted curves to the peak measurements and to the steady-state values are shown as solid or stippled lines,

respectively. See Table 1 for individual peak and steady-state potency values for each compound (IC_{50}, $logIC_{50}$ with 95% confidence intervals and N numbers).

Surprisingly, all compounds were able to inhibit $\alpha_1\beta_3\gamma_2$ $GABA_A$Rs even if complete inhibition was rarely achieved at the maximum solubility of 100 µM, especially for the peak measurements (Figure 5B-E). When assessing the mean potency IC_{50} peak values (Table 1), these ranged from 10 µM to 671 µM (ANOVA on $logIC_{50}$'s: $F_{14,64} = 6.2$, $p < 0.0001$), whereas the steady-state IC_{50} values varied from 10 µM to 73 µM (ANOVA on $logIC_{50}$'s: $F_{14,64} = 6.2$, $p < 0.0001$). On $\alpha_1\beta_3\gamma_2$ $GABA_A$Rs, PS has an IC_{50} around 1 µM,[34] hence, all the compounds in this study had potencies which were a least 10-fold lower than PS. Compound **4**, displayed the highest potency of all, followed by **1c**, **1b**, **3e** and **3f** as some of most potent ligands (Table 1). These five compounds displayed a complete inhibition at our maximum concentration of 100 µM.

Table 1. Data summary of inhibitory potencies from $\alpha1\beta3\gamma2$ $GABA_A$R at peak and steady state currents for all compounds tested (from mean inhibition curves shown in Figure 5B–E). Mean $LogIC_{50}$ values are shown with 95% confidence intervals (CI), of the number of experiments (N). IC_{50} values were calculated from the mean $LogIC_{50}$ values ($pIC_{50} = -\log IC_{50}$).

Cmpd	Measurement	IC_{50} (µM)	pIC_{50} (95% CI)	N
PS	Peak	292	-3.54 (-2.75, -4.32)	4
	Steady state	3.2	-5.49 (-5.31, -5.67)	4
1a	Peak	114	-3.94 (-4.14, -3.55)	8
	Steady state	23	-4.64 (-4.74, -4.54)	4
1b	Peak	29	-4.53 (-4.62, -4.46)	8
	Steady state	14	-4.84 (-4.90, -4.78)	8
1c	Peak	15	-4.84 (-4.94, -4.73)	4
	Steady state	12	-4.94 (-5.04, -4.84)	4
2a	Peak	55	-4.26 (-4.37, -4.15)	7
	Steady state	18	-4.73 (-4.83, -4.65)	4

2b	Peak	59	-4.23 (-4.45, -3.88)	4
	Steady State	14	-4.87 (-4.98, -4.75)	4
2c	Peak	190	-3.72 (-4.01, -3.06)	6
	Steady state	53	-4.28 (-4.82, -0.54)	4
2d	Peak	148	-3.83 (-4.00, -3.58)	4
	Steady State	73	-4.14 (-4.36, -3.76)	4
3a/b	Peak	671	-3.17 (-3.73, -1.49)	4
	Steady State	64	-4.19 (-4.29, -4.08)	4
3c	Peak	49	-4.31 (-4.37, -4.25)	10
	Steady state	24	-4.62 (-4.68, -4.57)	5
3d	Peak	54	-4.27 (-4.43, -4.06)	7
	Steady state	47	-4.32 (-4.46, -4.19)	6
3e	Peak	27	-4.57 (-4.74, -4.40)	4
	Steady state	21	-4.68 (-4.83, -4.54)	4
3f	Peak	37	-4.43 (-4.56, -4.26)	5
	Steady state	20	-4.70 (-4.82, -4.58)	5
3g	Peak	76	-4.12 (-4.30, -3.85)	4
	Steady state	42	-4.38 (-4.50, -4.26)	4
3h	Peak	128	-3.89 (-4.01, -3.70)	4
	Steady state	54	-4.27 (-4.35, -4.19)	4
4	Peak	10	-4.98 (-5.06, -4.90)	5
	Steady state	10	-5.00 (-5.06, -4.95)	5

In addition, when making multiple comparisons in Tukey's post hoc tests of pIC_{50} values, there was no obvious sign that C3 hydroxylated or C3 sulfated compounds differed in their potencies, neither from peak nor from steady-state measurements. However, compound **4**, which overall displayed the highest inhibitory potencies, was indeed based on the inhibitory NAS, PS; but since the IC_{50}'s for both peak and steady-state were identical for **4** (10 µM; and they differed for PS with much higher potency for inhibiting the steady state current compared to the peak current), it is doubtful that this compound binds to the exact same binding site as PS, or indeed exerts its inhibitory effect via a similar mechanism.

To further explore the nature of the C3 group on non-steroidal functionality, we selected two compounds, **1b** (C3 hydroxyl) and **1c** (C3 sulfate), with structures that only differed regarding the C3 group, and which had very similar pIC_{50} values for both peak and steady-state inhibition.

C3 sulfated NASs are generally inhibitory, whereas potentiating NASs usually carry a C3 hydroxyl group. Even if the orientation of the C3 hydroxyl group normally confers a PAM or NAM effect on NASs, it is feasible that the binding (and resulting function) of **1b** and **1c** on $GABA_A$ receptors might segregate with the mutation which consistently disrupts potentiating NASs binding and function, i.e. $\alpha 1^{Q241L}$.[35] Thus, we hypothesized that the binding (and effect) of **1b** might potentially be affected by this mutation as the molecule may bind similarly to pregnanolone, whereas the sulfated **1c** should not be affected, and might have a preference for the PS binding site. We observed that whereas the direct activations evoked by the two molecules were unchanged on wild-type $\alpha_1\beta_3\gamma_2$ and $\alpha_1^{Q241L}\beta_3\gamma_2$ (Figure 6B), the inhibition of the peak current was indeed significantly reduced on the mutant receptor for **1b** ($t_{(22)} = 12$, $p < 0.0001$), but not for **1c** ($t_{(12)} = 0.59$, $p = 0.56$; Figure 4a,c). Also, the steady-state level inhibition was unaffected by the α_1^{Q241L} mutation for both compounds (Figure 6A, D). This indicates that the binding and/or effect of **1b** might indeed be linked to the α_1^{Q241L} residue.

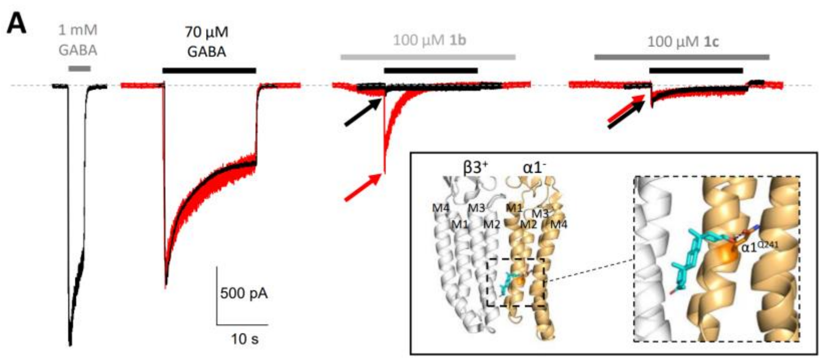

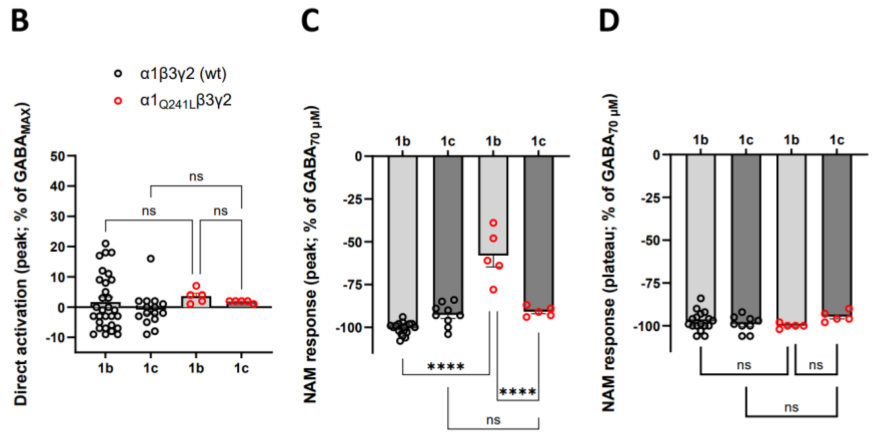

Figure 6. Assessment of α_1^{Q241} in the function of the two pure negative allosteric modulators, **1b** and **1c**. (A) Representative HEK cell current recordings from recombinant $\alpha_1\beta_3\gamma_2$ (black traces) or $\alpha_1^{Q241L}\beta_3\gamma_2$ (red traces) displaying responses to 70 μM GABA (~ EC80) with and without pre-applied compound **1b** (light grey) or **1c** (dark grey; both 100 μM). Insert: Representation of the binding of pregnanolone (C: cyan; O: red) to the outside-face of a $\beta_3^+\alpha_1^-$ interface (based on chimeric β_3(ECD)α_5(TMD)-homopentamer; PDB: 5O8F). The wildtype α_1^{Q241}(murine)- residue is highlighted (C: orange; O: red; N: blue) along with a proposed H-bond (black; stippled) formed with the C3α hydroxyl in ring A of pregnanolone. Histograms showing the lack of direct activation, (B) the inhibition of the peak current, (C) and the lack of effect of Q241 on the inhibition of the plateau (steady-state) current level, (D) of **1b** (light grey) or **1c** (dark grey). Individual values from $\alpha_1\beta_3\gamma_2$ (wildtype; wt) and $\alpha_1^{Q241L}\beta_3\gamma_2$ are shown as black or red circles, respectively. Mean percentage values are shown with SEM error bars, and statistical results from one-way ANOVA Tukey's multiple comparison tests are indicated where relevant (ns: not significant; ****: $p < 0.0001$).

We next assessed if any of the compounds were able to potentiate low GABA activation of the receptor (0.3 μM; ~ EC_{10} on $\alpha_1\beta_3\gamma_2$), with the expectation that the NAS PAM-based compound was more likely to do this. It became evident that only a single compound mixture, **3a/b**, acted as a potentiator and was significantly more efficacious than all the other compounds (including **3g**, which also displayed a tendency as a potentiator), and indeed this compound mixture was based on shape similarity to pregnanolone (Figure 7A, B). However, from concentration-response experiments with **3a/b** as a potentiator, it became clear that the potency was quite low (pEC_{50} 3.98 ± 1.08, EC_{50} >100 µM; Figure 7C).

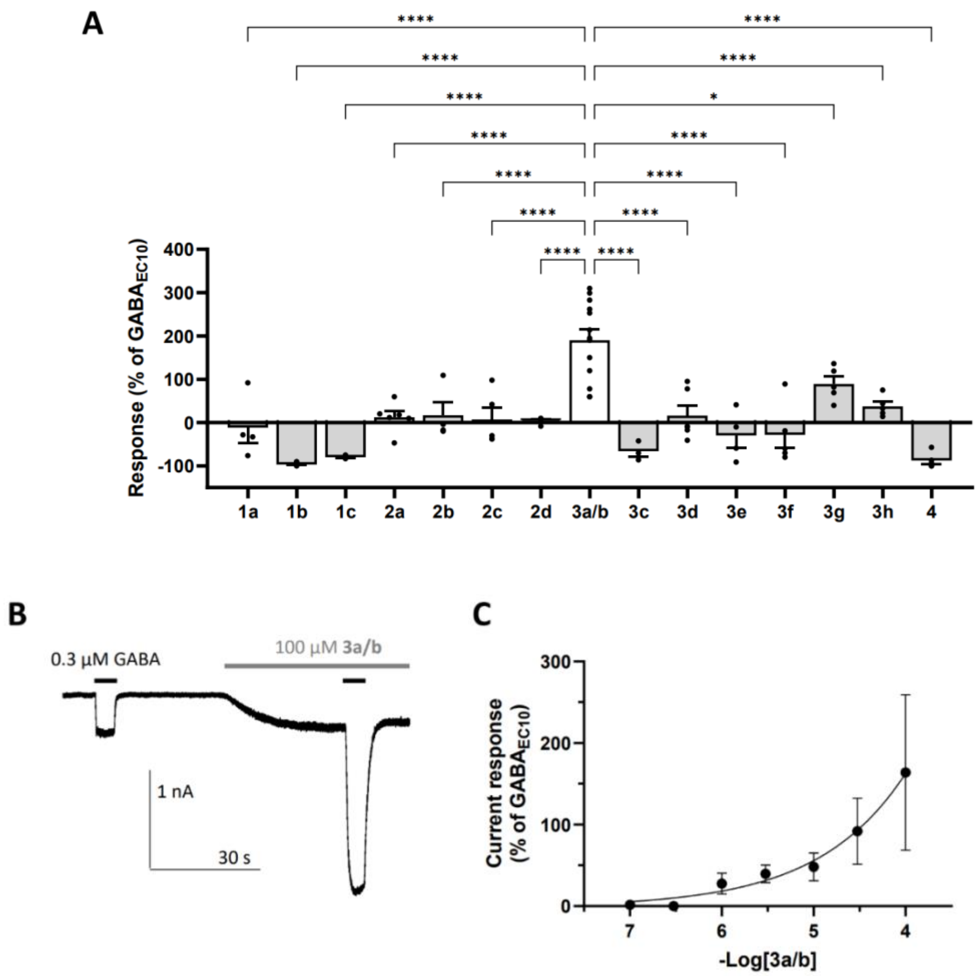

Figure 7. Positive allosteric effects on $GABA_A$Rs of compound **3a/b**. (A) histogram showing that only **3a/b** showed positive allosteric modulation of $\alpha_1\beta_3\gamma_2$ expressed in HEK cells (100 µM for all compound

with 0.3 µM GABA). The statistically significant results from a one-way ANOVA ($F_{14,70} = 17$, $p < 0.0001$) post hoc Tukey's multiple comparisons test is displayed (*: $p < 0.05$; ****: $p < 0.0001$). Note that compounds **1b** – **c**, **3c** and **4** (as the clearest examples) all exerted inhibition of the low activating GABA current (0.3 µM; ~ EC_{10}). (B) Representative current example highlighting the slow onset direct activation of 100 µM **3a/b** during pre-application, followed by a pronounced potentiation during co-application with 0.3 µM GABA. (C) concentration-response curve for **3a/b**. Note that due to a combination of a weak potency and a limited solubility of **3a/b**, only a partial concentration-response curve could be obtained (mean values ± SEM; N = 8).

As **3a/b** was a regioisomeric mixture, we separated the two isomers, as described previously, to evaluate if either was responsible for the potentiating effect of the mixture (Figure 8A). Subsequently, the regioisomeric mixture **3a/b**, and the two individual isomers **3a** and **3b**, were tested on both $\alpha_1\beta_3\gamma_2$ and $\alpha_1^{Q241L}\beta_3\gamma_2$ (Figure 8B, C, respectively). No statistical differences were observed in relevant pairwise comparisons when assessing the direct activation effects of **3a** and **3b** on either $\alpha_1\beta_3\gamma_2$ and $\alpha_1^{Q241L}\beta_3\gamma_2$ (Figure 8D). However, it became evident that the GABA potentiation effect of **3a/b** was induced only by the **3b** regioisomer with hardly any contribution to potentiation from **3a**. (Figure 8E).

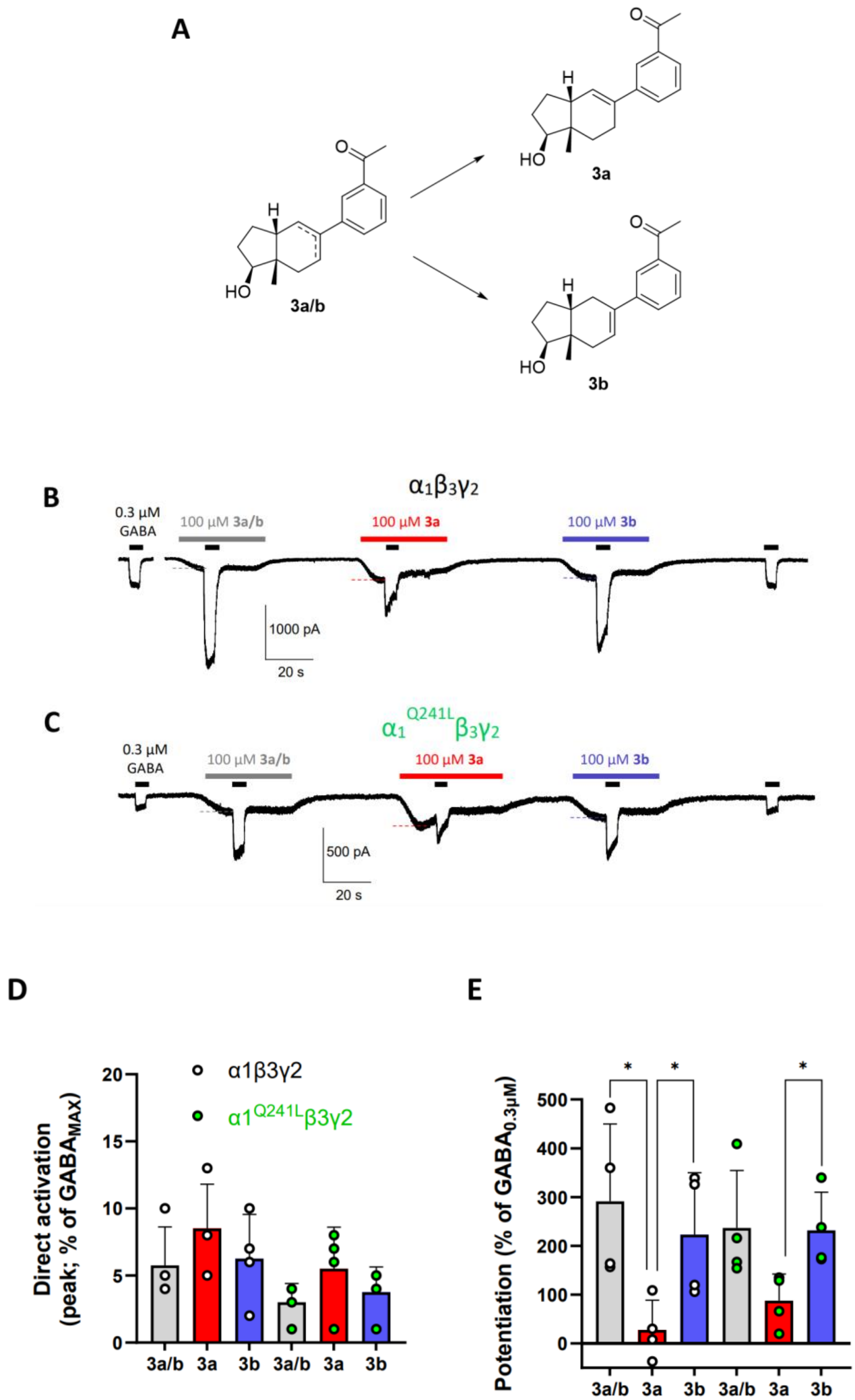

A
3a/b
3a
3b
HO
H
B
α1β3γ2
0.3 µM GABA
100 µM 3a/b
100 µM 3a
100 µM 3b
1000 pA
20 s
C
α1Q241Lβ3γ2
0.3 µM GABA
100 µM 3a/b
100 µM 3a
100 µM 3b
500 pA
20 s
D
α1β3γ2
α1Q241Lβ3γ2
Direct activation (peak; % of GABAMAX)
3a/b 3a 3b 3a/b 3a 3b
E
Potentiation (% of GABA0.3µM)
3a/b 3a 3b 3a/b 3a 3b

Figure 8. Search for the active $GABA_AR$-potentiating isomer in the regioisomeric mixture **3a/b**. Representative currents showing the direct activations and potentiating effects of **3a/b** (grey) and its two isomers, **3a** (red) and **3b** (blue), on $\alpha_1\beta_3\gamma_2$, A, and on $\alpha_1^{Q241L}\beta_3\gamma_2$, B. Note that the direct activation levels caused by the compounds are indicated by stippled lines. Histograms displaying the direct activation effects, C, and potentiating effects, D, of **3a/b**, **3a** and **3b**, on $\alpha_1\beta_3\gamma_2$ and on $\alpha_1^{Q241L}\beta_3\gamma_2$ where individual values are shown as white or green filled circles, respectively. Bars are mean values ± SEM. Only relevant statistical results from a one-way ANOVA Tukey's multiple comparisons test are displayed (*: $p < 0.05$), all other comparisons were not significant (not shown).

Surprisingly, the α_1^{Q241L} mutation did not significantly alter the potentiation profiles of **3a/b**, **3a** or **3b**, which indicates that neither of the regioisomers are likely to bind to a site overlapping or incorporating α_1^{Q241L} where potentiating NASs normally bind, unless different residues are involved. Hence, even if **3a** and **3b** were based on pregnanolone, their non-steroidal molecular structures seem sufficiently different from pregnanolone to precisely emulate its binding and effects.

Assessing the activity of compound 3b on native neuronal $GABA_ARs$.

Given the interesting profile of compound **3b** on recombinant receptors, we next assessed its activity on native neuronal $GABA_ARs$ using hippocampal neurons. Here, **3b** significantly potentiated the tonic holding current (Figure 9A,B) that underlies tonic inhibition confirming its activity as a PAM and further suggesting that **3b** may also target extrasynaptic-type $GABA_ARs$. The increased holding current induced by **3b** was maintained during the application of 30 μM **3b** and was also fully reversible (Figure 9A).

Corroborating evidence for **3b** as a PAM of neuronal $GABA_ARs$ can also be seen by the significantly prolonged sIPSC decay times, suggesting **3b** can also target synaptic receptors (e.g. $\alpha_1\beta_3\gamma_2$ as tested in the recombinant expression experiments). While the fast decay component of the sIPSCs remained largely unaltered in the presence of **3b**, the slow component was considerably prolonged by 10 µM **3b** (Figure 9C) with the mean sIPSC weighted decay time more than doubling (Figure 9D). Concurrently, 10 µM **3b** also reduced the sIPSC amplitude, notably with the larger synaptic events being ablated (Figure 9E, F). In addition, 10 µM **3b** did generate a trend towards decreasing sIPSC frequency, however, this was not statistically significant.

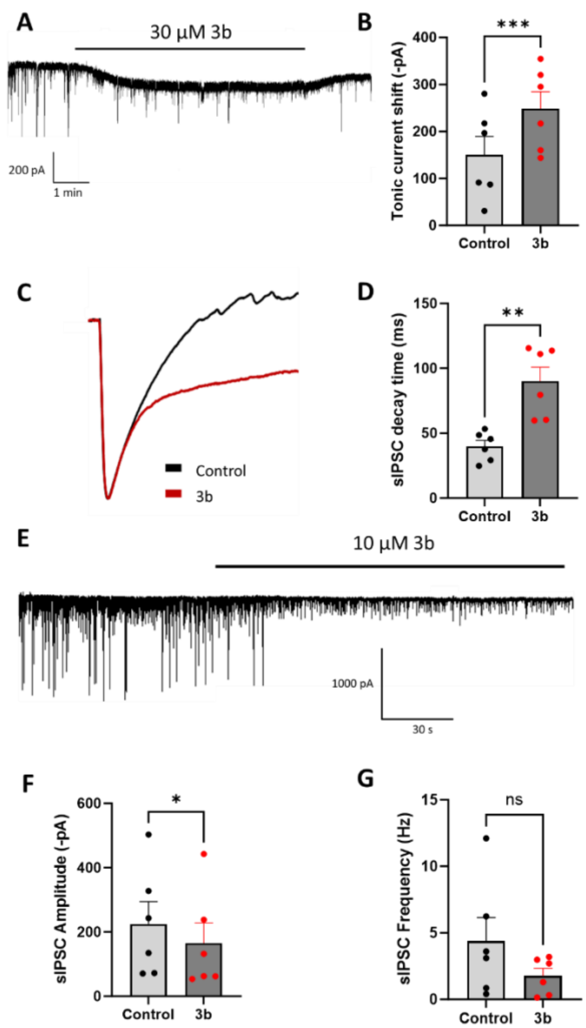

Figure 9. Assessing the activity of compound **3b** on native neuronal $GABA_A$Rs. (A) Representative whole-cell recording showing the effect of 30 µM **3b** on the membrane tonic current. (B) Bargraph showing the tonic current shift (-pA) in control neurons and in cells exposed to 30 µM **3b**. (C) Mean normalised sIPSC waveform example (from 60 to 300 events) showing the effect of 10 µM **3b** on prolonging the sIPSC decay time (ms; red trace) when compared to the control (black trace). (D) Bargraph for the effect of 10 µM **3b** on the sIPSC weighted decay time. Data points represent weighted tau values calculated using a bi-exponential curve fit to the sIPSC decay. (E) Representative whole cell recording depicting the change in sIPSC amplitude, but not frequency, in the presence of 10 µM **3b**. (F) Bargraph for the effect of 10 µM **3b** on reducing sIPSC amplitude (-pA). (F) Bargraph revealing little (not significant) effect of 10 µM **3b** on sIPSC frequency (Hz). Mean and individual values are shown with SEM. Statistical analysis of the results used paired t-tests where relevant with ns: not significant; and *** $p < 0.001$ for N = 6.

Discussion

In this study we aimed to identify, synthesize and pharmacologically characterize a series of non-steroidal analogues based on the molecular scaffold of the endogenous NASs, pregnanolone and PS. These non-steroidal derivatives were synthesized lacking one of the four aliphatic rings normally present in pregnanolone and which provides a rigid molecular conformation.

Four series of tricyclic non-steroidal compounds were synthesized with one compound based on a comparison with pregnanolone (**3b**), which in principle was expected to be a PAM, while the rest of the derivatives, based on the deconstruction of PS, were predicted to exhibit NAM-type profiles. Furthermore, only generic compounds in series **1** and **4** retained a relatively rigid ring structure (BCD and ABC, respectively) whilst compounds in series **2** and **3** were capable of rotational flexibility (ACD and ABD, respectively) which could affect the conformation of the C3 substituent which is considered a key residue for potentiating or inhibitory NAS-type activity at $GABA_A$Rs.

Of the 15 compounds examined for their direct activation potential of synaptic $GABA_A$Rs composed of $\alpha_1\beta_3\gamma_2$ subunits (synaptic isoform), only four compounds displayed significant activation compared to the maximum activation of the receptor by saturating GABA. Notably, all four compounds had a hydroxyl substituent at the C3 position in ring A, rather than the sulfate group from the parent PS structure. These four compounds, despite lacking one aliphatic ring and including an aromatic ring acted like potentiating NASs, such as THDOC, which induces direct $GABA_A$R activation at higher concentrations unlike inhibitory NASs.[3, 34, 35] Thus, these C3-OH non-steroidal ligands (with either a 5-member or 6-member ring A) displayed a 'PAM characteristic' despite all being derived from decomposition of the PS ring structure.

By contrast, the regioisomeric mixture **3a/b** based on the structural scaffold of pregnanolone, only display minimal direct receptor activation. Yet, in a further assessment of the non-steroidal compounds ability to potentiate GABA-induced currents, only **3a/b** (out of the 15 compounds) were capable of inducing a significant potentiation. Separation of the regioisomers into **3a** and **3b**, identified **3b** as the responsible compound for this effect. This result supported our approach of identifying non-steroidal compounds from the RCSB Protein Data Bank library by 'hopping' onto the scaffold of pregnanolone to find potentially new $GABA_A$R PAMs.

Given the structural similarity of the non-steroidal compounds (especially **3b**) to NASs and the discovery that some compounds acted as PAMs, it was interesting to find that the $\alpha 1^{Q241}$ in the $GABA_A$R was not crucial for the effect of **3b**. By contrast, this residue is essential for the binding of pregnanolone and other potentiating NASs.[4, 5, 36, 37] We predicted that due to the high level of structural similarity between the lead molecule PDB:5KRM and pregnanolone, that **3b** would likely bind to the same site as pregnanolone on $GABA_ARs$. However, it is conceivable that due to the greater flexibility of the non-steroid ring structure, the C3-hydroxyl group may be conformationally unable to participate in H-bonding to Q241 and instead, perhaps it is the hydrophobic interactions between the NAS binding site and the ABD ring system which engages **3b** ensuring its PAM effect. The alternative explanation of **3b**'s potentiating character is that it binds to a site distinct from the potentiating NASs, i.e. $\alpha1^{Q241}$. Further structure-based interrogation of the binding site for **3b** will help here.

For PS, we started the study on the assumption that it binds to a transmembrane site between M3 and M4 in the chimeric GLIC-$GABA_AR\alpha_1^{G258V}$ structure whilst also acknowledging that similar sites in other $GABA_AR$ subunits might also be important.[4] However, a recent cryo-EM study determined another binding site for PS in a recombinant $GABA_AR$ channel.[7] Because of this new finding, we decided not to examine the PS binding site fit of the new non-steroidal compounds, but instead to deconvolve the ring structure and substituents of the PS molecule and then examine the functionality of the new non-steroidal compounds.

Regarding our non-steroidal compounds based on PS deconstruction, all the compounds derived in this way retained some level of inhibition at recombinant $\alpha_1\beta_3\gamma_2$ $GABA_ARs$, with no obvious causality that could be attributed to the nature of the C3 substituent (hydroxyl, sulfate). However, a common factor linking all these non-steroidal compounds for inhibition of GABA currents, was their relatively low potency suggesting that chemical optimization might be beneficial. Compound **4**, which had the highest inhibitory potency in this set of molecules, was unique in carrying a bromo-group. This chemically-beneficial group could facilitate further optimization in the design of the non-steroidal compounds.

It was, however, interesting to observe that peak GABA current inhibition by one compound, **1b**, with a C3-OH, was reduced by the $GABA_AR$ α_1^{Q241L} mutation, whereas **1c**, harbouring a C3-sulfate substituent, was not. This was an unexpected finding suggesting that the α_1^{Q241} site, acknowledged to be important for the PAM effect of NASs, can also participate in inhibition by a non-steroidal compound with a C3-OH group.

The activity profile for compound **3b** on recombinant $GABA_AR$s suggested it should be active on native neuronal receptors. Using dissociated hippocampal neurons enabled the recording of both tonic and synaptic currents mediated by native $GABA_AR$s. This revealed **3b** modulation of both types of current implying binding and regulation by **3b** of synaptic and extrasynaptic $GABA_AR$s

For synaptic receptors, the modulatory profile was unusual with both an amplitude reduction and a profound prolongation of the sIPSC decay time, particularly affecting the slower component of the decay. Such a portfolio could arise from two distinct binding sites for **3b** on the synaptic $GABA_AR$ with one site causing antagonism (sIPSC amplitude reduction) and the other increasing the open probability of the ion channel (slow sIPSC decay rate), or alternatively, a single binding site may accommodate **3b** but it only causes incomplete partial inhibition that leaves the ion channel open for longer periods. Further analysis will be needed to distinguish between these PAM and NAM possibilities.

Our data also demonstrate that extrasynaptic neuronal $GABA_AR$s are sensitive to **3b**, with a two-fold increase in GABA-mediated tonic currents. This appears to be a pure PAM effect with no indication of inhibition. The receptors underlying tonic inhibition in the hippocampus are likely to be $\alpha_4\beta_3\delta$, $\alpha_5\beta_3\gamma_2$ and $\alpha_1\beta_3$, contrasting with the synaptic receptors of $\alpha_{1/2/3}\beta_{2/3}\gamma_2$. Because we observe a PAM and NAM effect on synaptic currents and just a PAM effect on tonic current, it suggests that **3b** is differentially regulating these receptor isoforms.

In conclusion, by adopting a shape similarity comparison in conjunction with chemicals logged in the PDB, we successfully synthesized and identified a novel non-steroidal $GABA_AR$ PAM (compound **3b**), and, by PS decomposition, we identified several $GABA_AR$ NAMs. This indicates the potential for using this methodology, in order to build a chemical library and also to identify non-steroidal ligand classes capable of modulating native $GABA_AR$s.

Experimental Section

Ligand preparation and shape similarity analysis. Protein complexes bound with steroids were chosen as reference proteins, encompassing the estrogen receptor complexed with estradiol (PDB: 1A52), the androgen receptor with dihydrotestosterone (PDB: 1T7T), the progesterone receptor with progesterone (PDB: 1A28), and the mineralocorticoid receptor bound with progesterone (PDB: 2AA5). A systematic structural alignment with these reference proteins was executed to analyze the binding mode and evaluate the ligand shape overlap between steroidal and non-steroidal ligands. Only non-steroidal ligands exhibiting appropriate overlap with the reference steroids were aggregated, yielding a collection of 34 non-steroidal ligands selected from RCSB Protein Data Bank (PDB). For the generation of bioactive conformers of the non-steroidal ligands, the Omega application from OpenEye Scientific Software was utilized. This led to a comprehensive set of multiple conformers for each non-steroidal ligand, which was subsequently employed as input for further ROCS calculations. Utilizing the $GABA_AR$ potentiating allosteric modulator, pregnanolone (5O8F) as the query molecule, Shape Tanimoto scores were determined and ranked, ultimately identifying 12 molecules with scores exceeding the set cutoff of 0.7, among which the hit compound in PDB (5KRM) achieved the highest score of 0.814.

Chemistry. *General procedures***.** All reagents and solvents were obtained from commercially available suppliers and used without further purification. Air / moisture sensitive reactions were carried out using flame-dry flasks and the syringe-septum technique under nitrogen / argon protection. Anhydrous DCM, THF and DMF were obtained from the solvent purification system (SPS), and the others were obtained from commercial suppliers or by storage over 3 Å or 4 Å molecular sieves. Thin layer chromatography (TLC) was carried out using Merck silica gel 60 F254 aluminium sheets and the detection was performed under UV light (254 nm) or $KMnO_4$ spray reagent. Flash column chromatography was performed using Merck silica gel (0.040 – 0.063 mm).

All compounds are >95% pure by HPLC analysis. Analytical high performance liquid chromatography was performed on a thermos scientific Dionex 3000 Ultimate instrument connected to a Gemini-NX C18 (250 × 4.6 mm) column and UV detection at 200, 210, 254 and 280 nm. Preparative HPLC was performed on a Thermos Scientific Dionex 3000 Ultimate instrument with a Gemini-NX RP C18 column (250 × 21.2 mm), an MWD-3000SD detector (254nm), a Rheodyne 9725i injector and an HPG-3200BX pump.

^{1}H and ^{13}C NMR spectrum were acquired using the 400 MHz Bruker Avance 400 MHz spectrometer equipped with a PABBO BB (^{1}H, ^{19}F) Z-GRD probe or a Bruker Avance 600 MHz spectrometer with a CPDCH ^{13}C(^{1}H) Z-GRD probe. The acquired NMR data are reported as follows: δ (chemical shift in ppm), s (singlet), d (doublet), t (triplet), q (quartet), m (multiplet), *J* (coupling constant in Hz), ROESY (Rotating frame Overhauser Effect Spectroscopy), COSY (Correlation Spectroscopy).

Mass spectra were acquired using ultra-performance liquid chromatography coupled with mass spectroscopy (UPLC-MS). This was executed on a Waters Acquity H-class UPLC system, integrating a Sample Manager FTN and a TUV dual wavelength detector, connected to a QDa single-quadrupole mass analyzer utilizing electrospray ionization. Chromatographic separation was achieved on an Acquity UPLC BEH C18 reversed-phase column (2.1 mm × 50 mm, 1.7 µm), maintained at 40 °C. A binary solvent gradient system was employed, transitioning from buffer A (Milli-Q H_2O, MeCN, and formic acid in a 95:5:0.1 v/v% ratio) to buffer B (MeCN and formic acid in a 100:0.1 v/v% ratio) over 3.5 minutes, followed by a 1 minute hold at 100% buffer B, at a flow rate of 0.8 mL/min. The acquisition and analysis of data were managed using Waters MassLynx software (version 4.1) and Waters OpenLynx browser (version 4.1), respectively.

General Procedure for Sulfonation. A mixture of the hydroxyl derivative (1 equiv) and sulfur trioxide pyridine complex (2 equiv) was dried in vacuo for 30 min and then dissolved in freshly dried chloroform (1 mL/10 mg), followed by addition of dry pyridine (1 drop). The reaction mixture was stirred at room temperature and the progress was monitored by analytic HPLC to ensure the full consumption of the hydroxyl starting material. When the reaction was finished, the resulting mixture was allowed to stand at -5 °C for 2 hours and then filtered. The filtrate was evaporated and dried in vacuo over 2 days to afford the corresponding sulfate.

2-((4a*R*,10a*R*)-4a-Methyl-3,4,4a,9,10,10a-hexahydrophenanthren-2(1*H*)-ylidene)ethan-1-ol (1a). Compound **10** (113 mg, 0.39 mmol, 1 equiv) was dissolved in anhydrous THF (5 mL) in 25 mL flame dry flask. DIBAL-H (1 M in THF, 3.9 mL, 3.9 mmol, 4 equiv) was added slowly at 0 °C and stirred at room temperature until full consumption of **10** determined by TLC. The reaction mixture was quenched by addition of Rochelles salt under vigorous stirring. The resulting mixture was diluted by DCM (40 mL) and washed by water (3 × 20 mL). The organic phase was dried over Na_2SO_4 and evaporated. The resulting crude was purified by prep-HPLC (MP: A, H_2O/TFA (100:0.1); B, ACN/H_2O/TFA (90/10/0.1)) using isocratic elution of 40% mobile phase B affording the diastereomer compound **1a** (60 mg, 62%) as a colorless oil. ^{1}H NMR (600 MHz, Chloroform-*d*): δ 7.30 – 7.27 (m, 1H), 7.17 – 7.13 (m, 1H), 7.09 – 7.04 (m, 1H), 7.04 – 7.01 (m, 1H), 5.42 – 5.39 (m, 1H), 3.59 – 3.51 (m, 2H), 2.82 – 2.75 (m, 1H), 2.70 – 2.64 (m, 1H), 2.29 – 2.24 (m, 1H), 2.21 – 2.14 (m, 2H), 2.09 – 1.99 (m, 2H), 1.92 – 1.84 (m, 1H), 1.75 – 1.59 (m, 3H), 1.29 (s, 3H). ^{13}C NMR (151 MHz, Chloroform-*d*): δ 143.6, 136.4, 134.4, 128.9, 128.3, 126.7, 126.1, 125.3, 60.1, 42.0, 40.5, 35.7, 35.0, 30.1, 27.7, 25.62, 25.60. UPLC-MS: m/z calculated $[M + H]^+$ for $C_{17}H_{23}O$ = 243.17 found 243.3.

(±)2-((4a*R*,10a*R*)-4a-Methyl-1,2,3,4,4a,9,10,10a-octahydrophenanthren-2-yl)ethan-1-ol (1b) Compound **11** was prepared in the same manner as **3e**. Starting from **10** (560 mg, 1.94 mmol, 1 equiv), compound **11** was yielded as a mixture of diastereomers without further purification. **1b** (147 mg, 61%) was prepared from **11** (350 mg) according to the procedure of **1a** in the mixture of diastereomers as a colorless oil in the ratio 11:19 analyzed by ^{1}H NMR. ^{1}H NMR (400 MHz, Chloroform-*d*): δ Major: 7.30 – 7.26 (m, 1H), 7.16 – 7.02 (m, 3H), 3.66 – 3.60 (t, 2H), 2.95 – 2.79 (m, 2H), 2.45 – 0.72 (m, 12H), 1.17 (s, 3H). Minor: 7.30 – 7.26 (m, 1H), 7.16 – 7.02 (m, 3H), 3.74 – 3.69 (t, 2H), 2.77 – 2.68 (m, 2H), 2.45 – 0.72 (m, 13H), 1.36 (s, 3H). ^{13}C NMR (101 MHz, Chloroform-*d*) could not be clearly assigned and is listed as below: δ 142.7, 135.9, 129.5, 125.9, 125.5, 125.2, 60.8, 41.3, 40.0, 38.2, 37.6, 34.8, 34.7, 34.1, 29.5, 25.3, 23.8. UPLC-MS: m/z calculated $[M + H]^+$ for $C_{17}H_{25}O$ = 245.19 found 245.1.

(±)2-((4a*R*,10a*R*)-4a-Methyl-1,2,3,4,4a,9,10,10a-octahydrophenanthren-2-yl)ethyl sulfate pyridinium (1c). Compound **1c** was prepared according to the general procedure for sulfonation. Starting from compound **1b** (20 mg, 0.08 mmol, 1 equiv), compound **1c** (29 mg, 88%) was obtained in a mixture of diastereomers as a colorless oil in the ration 11:19 analyzed by ^{1}H NMR. ^{1}H NMR (600 MHz, Chloroform-*d*): Major: 8.92 (d, *J* = 5.55 Hz, 2H), 8.47 – 8.43 (m, 1H), 7.95 (t, *J* = 6.62 Hz, 2H), 7.27 – 7.26 (m, 1H), 7.14 – 7.01 (m, 3H), 4.23 – 4.11 (m, 2H), 2.91 – 2.75 (m, 2H), 2.40 – 1.46 (m, 12H), 1.15 (s, 3H). Minor: 8.92 (d, *J* = 5.55 Hz, 2H), 8.47 – 8.43 (m, 1H), 7.95 (t, *J* = 6.62 Hz, 2H), 7.27 – 7.26 (m, 1H), 7.14 – 7.01 (m, 3H), 4.23 – 4.11 (m, 2H), 2.73 – 2.68 (m, 2H), 2.40 – 1.46 (m, 12H), 1.34 (s, 3H). ^{13}C NMR (151 MHz, Chloroform-*d*) could not be clearly assigned and is listed as below: δ 145.5, 142.8, 142.4, 135.9, 135.8, 129.5, 129.0, 126.8, 125.9, 125.8, 125.5, 125.2, 125.1, 60.8, 66.6, 41.2, 38.1, 37.5, 36.9, 36.4, 34.6, 34.5, 34.1, 29.0, 28.8, 26.0, 25.2, 23.8. UPLC-MS: m/z calculated $[M - H]^-$ for $C_{17}H_{23}O_4S$ = 323.13 found 323.2.

(1*S*,4*S*)-4-(2,3-Dihydro-1*H*-inden-5-yl)cyclohexan-1-ol (2a). (1*R*,4*R*)-4-(2,3-Dihydro-1*H*-inden-5-yl)cyclohexan-1-ol (2b). To the solution of 5-bromo-2,3-dihydro-1H-indene (333 mg, 1.69 mmol, 1 equiv) in anhydrous THF (5 mL) was added the solution of 1.6 M *n*-BuLi in THF (2.11 mL, 3.38 mmol, 2 equiv) dropwise at -78° C. LC-MS was used to ensure the consumption of 5-bromo-2,3-dihydro-1H-indene before addition of 4-((tert-butyldimethylsilyl)oxy)cyclohexan-1-one (385 mg, 1.69 mmol, 1 equiv) in anhydrous THF (2 mL) dropwise. The reaction mixture was stirred at this temperature for an additional 1.5 h, followed by quenching with NH_4Cl solid. After warming to room temperature, the mixture was diluted with water (10 mL) and extracted with ethyl acetate (3 × 10 mL). The organic phase was dried over Na_2SO_4, filtered and evaporated without further purification to afford **12** as a crude. The solution of the crude residue in 1M HCl ethanol was stirred at room temperature for 5 h. The reaction mixture was neutralized by saturated $NaHCO_3$ solution, extracted by ethyl acetate and dried over anhydrous Na_2SO_4, filtered and evaporated in vacuo. The crude dry precipitate was re-dissolved in ethanol, followed by addition of Pd/C (5% w/w, 20 mg). The resulting mixture was stirred under hydrogen atmosphere at room temperature and monitored by TLC. The crude was purified by silica gel chromatography (EtOAc/Heptane = 1:7) to yield compound **2a** (65 mg, 61%) as a white solid. ^{1}H NMR (400 MHz, Chloroform-*d*): δ 7.14 (d, *J* = 7.99, 1H), 7.09 – 7.08 (m, 1H), 6.97 (d, *J* = 7.56, 1H), 3.73 – 3.63 (m, 1H), 2.91 – 2.83 (m, 4H), 2.52 – 2.41 (m, 1H), 2.13 – 2.01 (m, 4H), 1.95 – 1.88 (m, 2H), 1.95 – 1.37 (m, 4H) ^{13}C NMR (101 MHz, Chloroform-*d*): δ 144.5, 144.4, 141.9, 124.6, 124.2, 122.7, 70.7, 43.3, 36.0, 32.8, 32.7, 32.4, 25.4. UPLC-MS: m/z calculated $[M + H]^+$ for $C_{15}H_{21}O$ = 217.16 found

217.2. Compound **2b** (15 mg, 14%) as a white solid. 1H NMR (600 MHz, DMSO) δ 7.09 (d, *J* = 7.7 Hz, 1H), 7.06 (d, *J* = 1.6 Hz, 1H), 6.94 (dd, *J* = 7.7, 1.6 Hz, 1H), 4.52 (d, *J* = 4.3 Hz, 1H), 3.43 (tq, *J*= 10.8, 4.3 Hz, 1H), 2.79 (dt, *J* = 9.9, 7.4 Hz, 4H), 2.38 (tt, *J* = 12.6, 3.5 Hz, 1H), 1.97 (p, *J* = 7.4 Hz, 2H), 1.92 – 1.86 (m, 2H), 1.75 – 1.68 (m, 2H), 1.49 – 1.39 (m, 2H), 1.26 (tdd, *J* = 12.7, 10.7, 3.5 Hz, 2H). ^{13}C NMR (101 MHz, DMSO-*d*$_6$): δ 146.0, 144.1, 141.4, 125.0, 124.4, 122.9, 63.8, 43.6, 33.3, 32.8, 32.4, 28.4, 25.6. UPLC-MS: m/z calculated $[M+H]^+$ for $C_{15}H_{21}O$ = 217.16 found 217.2.

(1*S*,4*S*)-4-(2,3-Dihydro-1*H*-inden-5-yl)cyclohexyl hydrogen sulfate pyridinium (2c). Compound **2c** was prepared according to the general procedure for sulfonation. Starting from compound **2a** (10 mg, 0.04 mmol, 1 equiv), compound **2c** (17 mg, 97 %) was obtained as a white solid. ^{1}H NMR (600 MHz, Chloroform-*d*): δ 8.89 – 8.84 (m, 2H), 8.43 – 8.36 (m, 1H), 7.93 – 7.87 (m, 2H), 7.08 – 7.03 (m, 2H), 6.95 – 6.90 (m, 1H), 4.83 – 4.78 (m, 1H), 2.83 – 2.76 (m, 4H), 2.49 – 2.40 (m, 1H), 2.30 – 2.22 (m, 2H), 2.02 – 1.93 (m, 2H), 1.92 – 1.80 (m, 2H), 1.65 – 1.52 (m, 4H). ^{13}C NMR (151 MHz, Chloroform-*d*): δ 145.5, 144.2, 142.1, 141.7, 127.0, 124.8, 124.0, 122.9, 74.5, 65.6, 43.5, 32.8, 32.4, 31.2, 29.7, 28.4, 28.0, 25.4. UPLC-MS: m/z calculated $[M - H]^-$ for $C_{15}H_{19}O_4S$ = 295.10 found 295.0.

(1*R*,4*R*)-4-(2,3-Dihydro-1*H*-inden-5-yl)cyclohexyl hydrogen sulfate pyridinium (2d). Compound **2d** was prepared according to the general procedure for sulfonation. Starting from compound **2b** (7 mg, 0.03 mmol, 1 equiv), compound **2d** (10 mg, 82%) was obtained as a white solid. ^{1}H NMR (600 MHz, Chloroform-*d*): δ 8.86 – 8.83 (m, 2H), 8.43 – 8.38 (m, 1H), 7.93 – 7.88 (m, 2H), 7.08 – 7.05 (m, 1H), 7.01 – 6.98 (m, 1H), 6.91 – 6.87 (m, 1H), 4.51 – 4.42 (m, 1H), 2.80 (q, *J* = 6.55 Hz, 4H), 2.47 – 2.28 (m, 3H), 2.03 – 1.94 (m, 4H), 1.90 – 1.83 (m, 2H), 1.60 – 1.45 (m, 4H). ^{13}C NMR (151 MHz, Chloroform-

d): δ 144.6, 143.4, 143.3, 141.1, 126.0, 123.6, 123.2, 121.7, 77.3, 42.1, 35.0, 32.2, 31.8, 31.7, 31.4, 30.9, 28.6, 24.4. UPLC-MS: m/z calculated $[M - H]^-$ for $C_{15}H_{19}O_4S$ = 295.10 found 295.0.

1-(3-((1*S*,3a*R*,7a*S*)-1-Hydroxy-7a-methyl-2,3,3a,6,7,7a-hexahydro-1*H*-inden-5-yl)phenyl)ethan-1-one (3a), 1-(3-((1*S*,3a*R*,7a*S*)-1-Hydroxy-7a-methyl-2,3,3a,4,7,7a-hexahydro-1*H*-inden-5-yl)phenyl)ethan-1-one (3b). To the solution of 2-(3-bromophenyl)-2-methyl-1,3-dioxolane (350 mg, 1.44 mmol, 2 equiv) in anhydrous THF (7 mL) was added the solution of 1.6 M *n*-BuLi in THF (0.92 mL, 1.47 mmol, 2 equiv) dropwise at -78° C. LC-MS was used to ensure the consumption of 2-(3-bromophenyl)-2-methyl-1,3-dioxolane before addition of **18** (208 mg, 0.73 mmol, 1 equiv) in anhydrous THF (2 mL) dropwise. The reaction mixture was stirred at this temperature for an additional 1.5 h, followed by quenching with NH_4Cl solid. After warming to room temperature, the mixture was diluted with water (10 mL) and extracted with ethyl acetate (3 × 10 mL). The organic phase was dried over Na_2SO_4, filtered and evaporated, yielding **19a** as a crude compound without further purification. To the crude compound **19a** (325 mg) in ethanol (5 mL) was added 5 mL 2 M HCl solution dropwise. The resulting mixture was stirred at room temperature and monitored by TLC to ensure the full consumption of starting material. The reaction mixture was neutralized by $NaHCO_3$ and diluted by water (20 mL) and extracted by ethyl acetate (3 × 15 mL). The combined organic phase was evaporated in vacuo and the crude mixture was purified by silica gel chromatography (Heptane/EtOAc 1:1) resulting in the product **3a/b** (156 mg, 79%) as a mixture of **3a** and **3b** isomers (^{1}H NMR integration ratio 7:3). Separation of the two isomers was performed using Daicel ChiralPAK AD column (250 mm x 20 mm) with isocratic Heptane:EtOH:TFA (80:20:0.1). (Figure S4) **3a**: ^{1}H NMR (600 MHz, DMSO-*d*$_6$) δ 7.92 (t, *J* = 1.8 Hz, 1H), 7.83 – 7.77 (m, 1H), 7.69 – 7.64 (m, 1H), 7.46 (t, *J* = 7.7 Hz, 1H), 6.21 – 6.17 (m, 1H), 4.47 (brs, 1H), 3.69 (t, *J* = 6.1 Hz, 1H), 2.59 (s, 3H), 2.42–2.36 (m, 2H), 2.35 – 2.28 (m, 1H), 2.13 – 2.03 (m, 1H), 2.00 – 1.91 (m, 1H), 1.59 – 1.46 (m, 2H), 1.45 – 1.38 (m, 1H), 1.32 – 1.24 (m, 1H), 0.91 (s, 3H). ^{13}C NMR (151 MHz, DMSO-*d*$_6$) δ 198.05, 141.81, 136.84, 132.69, 129.66, 129.37, 128.60, 126.35, 124.19, 76.45, 43.95, 41.77, 31.56, 29.86, 28.40, 26.76, 23.50, 19.75. UPLC-MS: m/z calculated $[M + H]^+$ for $C_{18}H_{23}O_2$ = 271.17, found = 271.2. **3b**: ^{1}H NMR (600 MHz, DMSO-*d*$_6$) δ 7.93 (t, *J* = 1.8 Hz, 1H), 7.83 – 7.78 (m, 1H), 7.70 – 7.65 (m, 1H), 7.46 (t, *J* = 7.7 Hz, 1H), 6.21 – 6.16 (m, 1H), 4.44 (d, *J* = 4.7 Hz, 1H), 3.64 – 3.59 (m, 1H), 2.59 (s, 3H), 2.53 – 2.47 (m, 1H), 2.33 – 2.26 (m, 1H), 2.14 – 2.04 (m, 2H), 1.96 – 1.88 (m, 1H), 1.82 – 1.72 (m, 2H), 1.47 – 1.38 (m, 1H), 1.30 – 1.20 (m, 1H), 0.93 (s, 3H). ^{13}C NMR (151 MHz, DMSO-*d*$_6$) δ 198.06, 141.91, 136.85, 132.68, 129.32, 128.60, 126.36, 124.13, 123.60, 78.10, 41.75, 39.27, 32.55, 31.43, 27.96, 27.09, 26.76, 20.38. UPLC-MS: m/z calculated $[M + H]^+$ for $C_{18}H_{23}O_2$ = 271.17, found = 271.2.

The mixture of (1*S*,3a*R*,7a*S*)-7a-Methyl-5-phenyl-2,3,3a,4,7,7a-hexahydro-1*H*-inden-1-ol and (1*S*,3a*R*,7a*S*)-7a-methyl-5-phenyl-2,3,3a,6,7,7a-hexahydro-1*H*-inden-1-ol (3c). The compound **19b** was prepared in the same manner as **19a**. Starting from **18** (300 mg, 1.05 mmol, 1 equiv) and bromobenzene (333 mg, 2.1 mmol, 2 equiv), **19b** was obtained as a crude compound for the next step without purification by silica gel chromatography. To the crude compound **19b** in ethanol (5 mL) was added 5 mL 2 M HCl solution dropwise. The resulting mixture was stirred at room temperature and monitored by TLC to ensure the full consumption of starting material. The reaction mixture was neutralized by $NaHCO_3$ and diluted by water (20 mL) and extracted by ethyl acetate (3 × 15 mL). The combined organic phase was evaporated in vacuo and the crude compound was purified by silica gel chromatography (Heptane/EtOAc 1:1) resulting in the mixture of **3c** (^{1}H NMR integration ratio Δ5,6: Δ4,5 = 11:19) (113 mg, 47% in two steps) as a colorless oil. ^{1}H NMR (400 MHz, Chloroform-*d*) Major: δ 7.41 – 7.37 (m, 2H), 7.33 – 7.29 (m, 2H), 7.23 – 7.20 (m, 1H), 6.09 – 6.05 (m, 1H), 3.92 – 3.87 (m, 1H), 2.46 – 2.36 (m, 2H), 2.28 – 2.10 (m, 2H), 1.93 – 1.79 (m, 1H), 1.66 – 1.26 (m, 5H), 1.02 (s, 3H). Minor: δ 7.41 – 7.37 (m, 2H), 7.33 – 7.29 (m, 2H), 7.23 – 7.20 (m, 1H), 6.05 – 6.00 (m, 1H), 3.84 – 3.79 (m, 1H), 2.46 – 2.36 (m, 2H), 2.28 – 2.10 (m, 2H), 1.93 – 1.79 (m, 1H), 1.66 – 1.26 (m, 5H), 1.05 (s, 3H).^{13}C NMR (101 MHz, Chloroform-*d*) could not be clearly assigned and is listed as below: δ 128.3, 128.2, 126.7, 125.0, 122.0, 80.5, 79.1, 44.3, 42.5, 42.4, 39.8, 32.7, 32.2, 31.9, 30.2, 29.0, 28.3, 27.3, 24.1, 22.7, 19.9, 19.3. UPLC-MS: m/z calculated $[M + H]^+$ for $C_{16}H_{21}O$ = 229.16, found = 229.2.

(1*S*,3a*R*,7a*S*)-7a-Methyl-5-phenyl-2,3,3a,4,7,7a-hexahydro-1*H*-inden-1-yl hydrogen sulfate pyridinium and (1*S*,3a*R*,7a*S*)-7a-Methyl-5-phenyl-2,3,3a,6,7,7a-hexahydro-1*H*-inden-1-yl hydrogen sulfate pyridinium (3d). Starting from compound **3c** (12 mg, 0.05 mmol, 1 equiv), **3d** was prepared according to the general procedure. (^{1}H NMR integration ratio Δ5,6: Δ4,5 = 11:19). ^{1}H NMR (400 MHz, Chloroform-*d*): Major: δ 8.98 – 8.90 (m, 2H), 8.50 – 5.41 (m, 1H), 8.01 – 7.92 (m, 2H), 7.40 – 7.35 (m, 2H), 7.32 – 7.27 (m, 2H), 7.23 – 7.17 (m, 1H), 6.04 – 6.01 (m, 1H), 4.69 – 4.64 (m, 1H), 2.59 – 1.32 (m, 9H), 1.10 (s, 3H). Minor: δ 8.98 – 8.90 (m, 2H), 8.50 – 5.41 (m, 1H), 8.01 – 7.92 (m, 2H), 7.40 – 7.35 (m, 2H), 7.32 – 7.27 (m, 2H), 7.23 – 7.17 (m, 1H), 6.04 – 6.01 (m, 1H), 4.61 – 4.57 (m, 1H), 2.59 – 1.32 (m, 9H), 1.10 (s, 3H). ^{13}C NMR (101 MHz, Chloroform-*d*) could not be clearly assigned and is listed as below: δ 145.6, 142.1, 128.1, 127.0, 126.6, 125.08, 125.03, 87.8, 44.4, 42.3, 40.4, 32.44, 30.0, 29.7, 28.7, 24.1, 20.4, 20.1. UPLC-MS: m/z calculated $[M - H]^-$ for $C_{16}H_{19}O_4S$ = 307.10 found 307.0.

(1*S*,3a*R*,5*R,7a*S*)-7a-Methyl-5-phenyloctahydro-1*H*-inden-1-ol (3e)**. To the solution of **3c** (40 mg, 0.17 mmol, 1 equiv) in methanol was added Pd/C (5% w/w on carbon, 5 mg). The reaction mixture was degassed three times (evacuated and backfilled with H_2) and stirred in the atmosphere of H_2 at room temperature for 1 h. The resulting mixture was filtered and evaporated in vacuo, followed by isolation of diastereomers through prep-HPLC (MP: A, H_2O/TFA (100: 0.1); B, ACN/H_2O/TFA (90/10/0.1)) using isocratic elution of 30% mobile phase B to give **3e** (18 mg, 44%) as a white solid. ^{1}H NMR (600 MHz, Chloroform-*d*): δ 7.31 – 7.27 (m, 2H), 7.24 – 7.22 (m, 2H), 7.20 – 7.16 (m, 1H), 3.74 (d, *J* = 5.76 Hz, 1H), 2.75 – 2.68 (m, 1H), 2.29 – 2.22 (m, 1H), 2.14 – 2.08 (m, 1H), 1.91 – 1.57 (m, 7H), 1.33 – 1.25 (m, 2H), 1.14 (s, 3H). ^{13}C NMR (151 MHz, Chloroform-*d*): δ 147.4, 128.4, 127.0, 125.9, 82.6, 44.1, 41.5, 38.2, 32.1, 32.0, 29.3, 26.6, 18.4, UPLC-MS: m/z calculated $[M + H]^+$ for $C_{16}H_{23}O$ = 231.17, found = 231.2.

(1*S*,3a*R*,5*S,7a*S*)-7a-Methyl-5-phenyloctahydro-1*H*-inden-1-ol (3f)**. Compound **3f** was prepared in the same manner as **3e**. Starting from **3c** (40 mg, 0.17 mmol, 1 equiv), compound **3f** was obtained by prep-HPLC (MP: A, H_2O/TFA (100: 0.1); B, ACN/H_2O/TFA (90/10/0.1)) using isocratic elution of 30% mobile phase B to give **3f** (6 mg, 15%) as a white solid. ^{1}H NMR (600 MHz, Chloroform-*d*): δ 7.32 – 7.26 (m, 2H), 7.21 – 7.15 (m, 3H), 4.39 (t, *J* = 8.76 Hz, 1H), 2.52 – 2.43 (m, 1H), 2.28 – 2.17 (m, 1H), 2.14 – 2.02 (m, 1H), 1.94 – 1.87 (m, 1H), 1.83 – 1.52 (m, 5H), 1.48 – 1.38 (m, 1H), 1.26 – 1.16 (m, 2H), 0.93 (s, 3H). ^{13}C NMR (151 MHz, Chloroform-*d*): δ 147.3, 128.3, 126.7, 125.9, 73.7, 45.1, 43.7, 42.7, 38.9, 33.1, 30.0, 29.3, 26.9, 22.1. UPLC-MS: m/z calculated $[M + H]^+$ for $C_{16}H_{23}O$ = 231.17, found = 231.2.

(1*S*,3a*R*,5*R,7a*S*)-7a-Methyl-5-phenyloctahydro-1*H*-inden-1-yl hydrogen sulfate pyridinium (3g).** Compound **3g** was prepared according to the general procedure for sulfonation. Starting from compound **3e** (10 mg, 0.04 mmol, 1 equiv), compound **3g** (11 mg, 65%) was obtained as a white solid. ^{1}H NMR (600 MHz, Chloroform-*d*): δ 8.97 – 8.94 (m, 2H), 8.49 – 8.45 (m, 1H), 8.00 – 7.97 (m, 2H), 7.30 – 7.26 (m, 2H), 7.23 – 7.20 (m, 2H), 7.19 – 7.15 (m, 1H), 4.52 (d, J = 5.59 Hz, 1H), 2.74 – 2.67 (m, 1H), 2.34 – 2.27 (m, 1H), 2.21 – 2.11 (m, 2H), 1.91 – 1.62 (m, 6H), 1.43 – 1.32 (m, 2H), 1.22 (s, 3H). ^{13}C NMR (151 MHz, Chloroform-*d*): δ 146.3, 144.6, 141.1, 127.2, 126.0, 125.9, 124.8, 89.1, 42.9, 41.1, 36.9, 30.9, 30.7, 28.9, 28.1, 25.4, 17.7. UPLC-MS: m/z calculated $[M - H]^-$ for $C_{16}H_{21}O_4S$ = 309.12 found 309.1.

(1*S*,3a*R*,5*S,7a*S*)-7a-Methyl-5-phenyloctahydro-1H-inden-1-yl hydrogen sulfate pyridinium (3h).** Compound **3h** was prepared according to the general procedure for sulfonation. Starting from compound **3f** (7 mg, 0.03 mmol, 1 equiv), compound **3h** (6 mg, 53%) was obtained as a white solid. ^{1}H NMR (151 MHz, Chloroform-*d*): δ 8.95 – 8.92 (m, 2H), 8.48 – 8.44 (m, 1H), 7.99 – 7.95 (m, 2H), 7.28 – 7.25 (m, 2H), 7.20 – 7.17 (m, 2H), 7.17 – 7.14 (m, 1H), 5.10 (t, J = 8.79 Hz, 1H), 2.49 – 2.38 (m, 2H), 2.14 – 2.07 (m, 2H), 1.97 – 1.91 (m, 2H), 1.82 – 1.66 (m, 3H), 1.42 – 1.35 (m, 1H), 1.31 – 1.21 (m, 2H), 1.00 (s, 3H). ^{13}C NMR (151 MHz, Chloroform-*d*): δ 147.4, 145.6, 142.1, 128.3, 127.1, 126.8, 125.8, 80.5, 44.6, 43.8, 42.8, 38.8, 32.9, 29.2, 27.3, 27.1, 23.1. UPLC-MS: m/z calculated $[M - H]^-$ for $C_{16}H_{21}O_4S$ = 309.12 found 309.1.

(2*S*,4a*S*)-7-Bromo-4a-methyl-1,2,3,4,4a,9-hexahydrophenanthren-2-yl hydrogen sulfate pyridinium (4). Compound **4** was prepared according to the general procedure for sulfate. Starting from compound **26** (20 mg, 0.08 mmol, 1 equiv), compound **4** (22 mg, 70%) was obtained as a white solid. ^{1}H NMR (600 MHz, DMSO-d_6): δ 8.86 – 8.82 (m, 2H), 8.42 – 8.37 (m, 1H), 7.92 – 7.87 (m, 2H), 7.37 – 7.26 (m, 3H), 5.57 – 5.53 (m, 1H), 3.94 – 3.84 (m, 1H), 3.36 – 3.31 (m, 2H), 2.60 – 2.55 (m, 1H), 2.30 – 2.25 (m, 1H), 2.22 – 2.14 (m, 1H), 2.04 – 1.96 (m, 1H), 1.72 – 1.60 (m, 1H), 1.39 – 1.32 (m, 1H), 1.29 (s, 3H). ^{13}C NMR (151 MHz, Chloroform-*d*): δ 144.3, 143.7, 143.3, 137.9, 135.0, 130.3, 129.1, 128.6, 126.6, 118.5, 118.3, 74.5, 40.1, 37.6, 36.8, 29.3, 28.9, 26.4. UPLC-MS: m/z calculated $[M - H]^-$ for $C_{15}H_{16}BrO_4S$ = 371.00 and 372.99 found 371.1 and 373.2.

(5*S*)-8-Hydroxy-5,8-dimethyl-5,6,7,8,9,10-hexahydro-5,9-methanobenzo[8]annulen-11-one (5). A solution of compound 1-methyl-3,4-dihydronaphthalen-2(1H)-one (6 g, 37.5 mmol) and *S*-(-)-α-methylbenzylamine (4.53 g, 37.5 mmol) in toluene was heated to reflux employing a Dean-Stark apparatus for water removal. The progress of the reaction was tracked by ^{1}H NMR until the complete consumption of 1-methyl-3,4-dihydronaphthalen-2(1H)-one. The solvent was then evaporated under reduced pressure. The residual material was re-dissolved in 100 mL THF, followed by the addition of freshly distilled methyl vinyl ketone (MVK, 2.86 g, 41.2 mmol). The resulting mixture was stirred continuously for 48 h. The reaction mixture was subsequently diluted with water (80 mL) and acetic acid (10 mL), and then extracted with ethyl acetate (EtOAc, 3 × 60 mL). The combined organic extracts were dried over Na_2SO_4 and concentrated under reduced pressure. Purification via silica gel chromatography (eluting with a gradient of EtOAc:heptane from 1:30 to 1:1) yielded compound **5** as brown crystals (6.46 g, 75% yield).^{1}H NMR (600 MHz, DMSO-d_6): δ 7.26 – 7.16 (m, 3H), 7.12 – 7.10 (m, 1H), 4.62 (s, 1H), 3.24 – 3.14 (m, 2H), 2.48 – 2.45 (m, 1H), 2.06 – 2.00 (m, 1H), 1.51 – 1.47 (m, 1H), 1.39 – 1.34 (m, 1H), 1.32 (s, 3H), 1.28 – 1.24 (m, 1H), 1.23 (s, 3H). ^{13}C NMR (151 MHz, DMSO-d_6): δ 213.6, 142.7, 134.3, 127.2, 126.9, 126.5, 125.0, 76.8, 56.7, 47.7, 40.0, 34.3, 32.0, 27.6, 19.9.

(*R*)-4a-Methyl-4,4a,9,10-tetrahydrophenanthren-2(3*H*)-one (6). To a solution of compound **5** (1.080 g, 4.69 mmol) in toluene (30 mL), *p*-toluenesulfonic acid (PTSA, 50 mg) was added. The reaction mixture was heated to reflux for 4 h. After that, the mixture was diluted with ethyl acetate (60 mL). The resultant organic layer was sequentially washed with saturated $NaHCO_3$ (15 mL) and brine (15 mL), then dried over Na_2SO_4. After concentration, purification was achieved via silica gel chromatography (eluting with EtOAc: heptane = 1:5) to afford compound **6** as a brown solid (632 mg, 63% yield). ^{1}H NMR (400 MHz, Chloroform-*d*): δ 7.32 – 7.28 (m, 1H), 7.25 – 7.21 (m, 1H), 7.18 – 7.12 (m, 1H), 7.11 – 7.08 (m, 1H), 5.92 – 5.89 (m, 1H), 3.06 – 1.98 (m, 1H), 2.95 – 2.85 (m, 1H), 2.77 – 2.64 (m, 2H), 2.58 – 2.48 (m, 2H), 2.42 – 2.35 (m, 1H), 2.42 – 2.12 (m, 1H), 1.58 (s, 3H). ^{13}C NMR (101 MHz, Chloroform-*d*): δ 198.9, 169.8, 143.8, 134.8, 128.6, 127.0, 126.2, 126.1, 124.2, 39.2, 36.9, 34.8, 31.22, 31.20, 27.7.

(*R*)-4a-Methyl-3,4,4a,9-tetrahydro-1*H*-spiro[phenanthrene-2,2'-[1,3]dioxolane] (7). To the solution of **6** (2.77 g, 13.06 mmol, 1 equiv) in toluene (80 mL) was added PTSA (6.3 mg) and ethylene glycol (4.86 g, 78.36 mmol, 6 equiv). The reaction mixture was heated to reflux with a Dean-Stark water trap until the starting material was fully consumed. The resulting mixture was diluted by saturated $NaHCO_3$ (40 mL) and extracted by ethyl acetate (3 × 50 mL). The combined organic phase was evaporated and the crude compound was purified by silica-gel chromatography (EtOAc: Heptane = 1:7) to yield **7** (1.58 g, 47%) as a colorless oil. ^{1}H NMR (400 MHz, Chloroform-*d*): δ 7.34 – 7.30 (m, 1H), 7.21 – 7.15 (m, 1H), 7.14 – 7.08 (m, 1H), 7.08 – 7.04 (m, 1H), 5.63 – 5.59 (m, 1H), 4.01 – 3.89 (m, 4H), 3.43 – 3.39 (t, *J* = 3.08 Hz, 2H), 2.76 – 2.68 (m, 1H), 2.32 – 2.26 (m, 1H), 2.19 – 2.13 (m, 1H), 2.07 – 1.96 (m, 1H), 1.86 – 1.77 (m, 2H), 1.41 (s, 3H). ^{13}C NMR (101 MHz, Chloroform-*d*): δ 142.7, 136.5, 131.4, 127.1, 125.1, 124.9, 124.6, 118.6, 107.7, 63.4, 63.3, 40.8, 36.3, 35.9, 30.7, 28.9, 25.4.

(4a*R*,10a*R*)-4a-Methyl-3,4,4a,9,10,10a-hexahydro-1*H*-spiro[phenanthrene-2,2'-[1,3]dioxolane] (8). To the solution of **7** (1.58 g, 6.16 mmol, 1 equiv) in toluene (20 mL) was added $Pd(OH)_2/C$ (20%, 160 mg). The resulting mixture was degassed four times (evaporated and backfilled with H_2) and then stirred in the high pressure of H_2 (50 psi) at 50 °C for 5 days. The reaction mixture was filtered, evaporated and purified by silica-gel chromatography (EtOAc: Heptane = 1:5) to yield **8** (900 mg, 56 %) as a colorless oil. ^{1}H NMR (600 MHz, Chloroform-*d*): δ 7.30 – 7.27 (m, 1H), 7.15 – 7.10 (m, 1H), 7.09 – 7.03 (m, 2H), 3.98 – 3.88 (m, 4H), 2.89 – 2.82 (m, 1H), 2.78 – 2.72 (m, 1H), 2.33 – 2.28 (m, 1H), 2.23 – 2.13 (m, 1H), 1.95 – 1.90 (m, 1H), 1.75 – 1.68 (m, 1H), 1.63 – 1.55 (m, 4H), 1.42 – 1.36 (m, 1H), 1.22

(s, 3H). ^{13}C NMR (151 MHz, Chloroform-*d*): δ 134.7, 128.5, 125.0, 124.5, 124.4, 108.6, 63.2, 63.1, 38.0, 35.8, 35.3, 34.0, 30.5, 24.5, 22.6, 21.7, 13.1.

(4a*R*,10a*R*)-4a-Methyl-3,4,4a,9,10,10a-hexahydrophenanthren-2(1*H*)-one (9). To the solution of **8** (900 mg, 3.67 mmol, 1 equiv) in ethanol (10 mL) was added 2M HCl (10 mL). The reaction mixture was stirred over 2 h followed by slow addition of $NaHCO_3$ solid till the pH reached 7. Ethyl acetate (3 × 15 mL) was added to extract the resulting solution and the combined organic phase was dried over Na_2SO_4, evaporated and purified by silica-gel chromatography (EtOAc/Heptane = 1:2) to yield **9** (677 mg, 90%) as a colorless oil. ^1H NMR (400 MHz, DMSO-d_6): δ 7.42 – 7.37 (m, 1H), 7.19 – 7.04 (m, 3H), 2.83 – 2.74 (m, 2H), 2.48 – 2.43 (m, 1H), 2.36 – 2.26 (m, 2H), 2.16 – 1.80 (m, 5H), 1.61 – 1.51 (m, 1H), 1.38 (s, 3H). ^{13}C NMR (101 MHz, DMSO-d_6): δ 210.8, 142.4, 134.9, 129.2, 126.1, 126.0, 125.6, 43.1, 41.8, 37.7, 36.8, 36.3, 29.0, 26.3, 24.4.

Ethyl 2-((4a*R*,10a*R*,E/*Z*)-4a-methyl-3,4,4a,9,10,10a-hexahydrophenanthren-2(1*H*)-ylidene) acetate (10). To a stirred suspension of NaH (55% in mineral oil, 182 mg, 3.79 mmol, 1.2 equiv) in anhydrous THF (5 mL) at 0 °C was added triethyl phosphonoacetate (850 mg, 3.79 mmol, 1.2 equiv) dropwise. The reaction was heated to 40 °C and stirred for 1 h. Compound **9** (677 mg, 3.16 mmol, 1.2 equiv) was added dropwise after cooling to 0 °C and then the resulting mixture was heated to 40 °C again and stirred for another 12 h. The reaction was quenched by slowing adding water (10 mL) and extracted with EtOAc (3 × 15 mL). The combined organic phase was dried over Na_2SO_4, evaporated and purified by silica-gel chromatography (EtOAc: Heptane = 1:1) to yield **10** (592 mg, 65%, E/Z ratio 34/66) as a colorless oil. ^1H NMR (600 MHz, $CDCl_3$) δ 7.35 – 7.27 (m, 1H), 7.17 – 7.12 (m, 1H), 7.11 – 6.99 (m, 2H), 5.45 (m, 1H), 4.19 – 4.10 (m, 0.68H), 4.06 (m, 1.33H), 3.03 – 2.88 (m, 2H), 2.88 – 2.75 (m, 1H), 2.70 – 2.62 (m, 1H), 2.28 – 2.20 (m, 1H), 2.07 – 1.96 (m, 3H), 1.89 – 1.73 (m, 1H), 1.73 – 1.57 (m, 2H), 1.31 – 1.23 (m, 3H), 1.34 – 1.14 (m, 6H).

^{13}C NMR (151 MHz, Chloroform-*d*): δ 170.7, 142.8, 135.5, 130.3, 128.2, 127.8, 125.7, 124.9, 124.1, 59.3, 42.1, 41.1, 34.4, 33.8, 28.7, 27.0, 25.1, 24.7, 13.1.

2-Methyl-2-(3-oxobutyl)cyclopentane-1,3-dione (13). To the suspension of 2-methyl-1,3-cyclopentanedione (2 g, 17.85 mmol, 1 equiv) in H_2O (10 mL) was added MVK (2.25 g, 32.14 mmol, 1.8 equiv) and HOAc (54 μL). The reaction flask was shielded from light and heated to 70 °C for 4 h. Upon cooling to room temperature, the mixture was extracted with DCM (3 × 10 mL). The combined organic layers were then evaporated to afford a light yellow oil, which was used in subsequent steps without further purification. ^{1}H NMR (400 MHz, Chloroform-*d*): δ 2.88 – 2.67 (m, 4H), 2.43 (t, *J* = 7.16, 2H), 2.07 (s, 3H), 1.86 (t, *J* = 7.26, 2H), 1.08 (s, 3H). ^{13}C NMR (101 MHz, Chloroform-*d*): δ 215.7, 207.8, 55.0, 37.4, 34.7, 30.0, 27.7, 19.0.

(*S*)-7a-Methyl-2,3,7,7a-tetrahydro-1*H*-indene-1,5(6*H*)-dione (15). The L-proline (60 mg, 0.52 mmol, 3% equiv) suspension in DMF (5 mL) was subjected to three cycles of degassing (evaporation and backfilling with N_2), stirred at 16 °C under light exclusion. The solution of compound **13** in DMF was then added to this mixture. Subsequently, the combined mixture was again degassed twice before returning to room temperature. The reaction mixture was stirred at room temperature, shielded from light, for four days, with progress monitored by TLC to confirm reaction completion. The resultant mixture **14** was carried to the next step without further processing. A solution of H_2SO_4 in DMF was prepared by dropwise addition of concentrated H_2SO_4 (0.5 mL) to DMF (9.1 mL) at -21 °C. The reaction mixture of **14** in DMF was heated to 75 – 80° C followed by addition of an aliquot H_2SO_4 solution (1.2 mL). Then the mixture was heated to 95° C and stirred for 1 h, followed by addition of another aliquot of H_2SO_4 in DMF (0.6 mL). The resulting mixture was then stirred for 3.5 h. The resulting mixture was diluted by water (20 mL) and extracted by EtOAc (3 × 15 mL). The combined organic phase was dried over Na_2SO_4 and evaporated. The crude residue was purified by silica gel chromatography (Hep/EtOAc = 2:1 to 1:1) to give **15** (1.42 g, 48%) as a colorless oil. ^{1}H NMR (151 MHz, Chloroform-*d*): δ 5.97 – 5.95 (m, 1H), 2.99 – 2.91 (m, 1H), 2.82 – 2.71 (m, 2H), 2.55 – 2.39 (m, 3H), 2.12 – 2.08 (m, 1H), 2.03 (s, 3H), 1.88 – 1.81 (m, 1H). ^{13}C NMR (151 MHz, Chloroform-*d*): δ 216.5, 198.1, 169.7, 123.9, 48.7, 35.9, 32.9, 29.2, 26.8, 20.6.

(1*S*,7a*S*)-1-Hydroxy-7a-methyl-1,2,3,6,7,7a-hexahydro-5*H*-inden-5-one (16). To the solution of **15** (1.424 g, 8.68 mmol, 1 equiv) in ethanol (22 mL) was added $NaBH_4$ (99 mg, 2.60 mmol, 0.3 equiv) in ethanol (16 mL) dropwise within 3.5 h at -18° C. The resulting mixture was stirred for another 1 h at this temperature, followed by quenching with HCl (2 M) slowly until pH reached 6. Then EtOAc (3 × 15 mL) was added for extraction. The combined organic phase was dried over Na_2SO_4, filtered and evaporated. The crude was purified by silica gel chromatography (EtOAc/Heptane = 1:2 to 1:1) to give **16** (1.056 g, 73%) as a colorless oil. ^{1}H NMR (600 MHz, DMSO-d_6): δ 5.65 – 5.56 (m, 1H), 5.00 (d, J = 4.98, 1H), 3.65 – 3.59 (m, 1H), 2.66 – 2.59 (m, 1H), 2.49 – 2.42 (m, 1H), 2.35 – 2.28 (m, 1H), 2.19 – 2.14 (m, 1H), 1.98 – 1.87 (m, 2H), 1.71 – 1.60 (m, 2H), 1.02 (s, 3H). ^{13}C NMR (151 MHz, DMSO-d_6): δ 197.9, 176.1, 122.3, 79.1, 44.8, 33.8, 33.0, 28.5, 26.0, 14.8.

(1*S*,3a*R*,7a*S*)-1-Hydroxy-7a-methyloctahydro-5*H*-inden-5-one (17). The solution of compound **16** (2 g, 12.04 mmol, 1 equiv) in anhydrous THF (10 mL) was introduced into liquid ammonia at -78 °C. This mixture was stirred for 1 h before a slow addition of solid NH_4Cl for quenching. Upon warming to room temperature, the reaction mixture was treated with water (20 mL) and ethyl acetate (15 mL), followed by additional extractions (2 × 15 mL). The combined organic extracts were dried over Na_2SO_4, filtered, and the solvent was evaporated. Purification by silica gel chromatography (EtOAc/Heptane = 1:1) afforded compound **17** (1.461 g, 72%) as a white solid.[1]H NMR (600 MHz, DMSO-d_6): δ 4.53 (d, *J* = 4.77, 1H), 3.69 – 3.65 (m, 1H), 2.44 – 2.39 (m, 1H), 2.37 – 2.31 (m, 1H), 2.12 – 2.04 (m, 3H), 1.98 – 1.92 (m, 1H), 1.81 – 1.75 (m, 1H), 1.63 – 1.57 (m, 1H), 1.52 – 1.47 (m, 1H), 1.46 – 1.39 (m, 1H), 1.09 – 1.05 (m, 1H), 1.04 (s, 3H). 13C NMR (151 MHz, DMSO-d_6): δ 212.1, 77.7, 43.4, 42.5, 41.9, 36.4, 31.7, 31.5, 28.0, 19.8.

(1*S*,3a*R*,7a*S*)-1-((tert-Butyldimethylsilyl)oxy)-7a-methyloctahydro-5*H*-inden-5-one (18). To the solution of **17** (1.1 g, 6.54 mmol, 1 equiv) and TBDMSCl (1.595 g, 10.56 mmol, 1.6 equiv) in DMF (8 mL) was added imidazole (1.182g, 17.28 mmol, 2.6 equiv). The reaction mixture was stirred at room temperature for 1 h and then diluted with EtOAc and washed with brine, water and dried over Na_2SO_4. After filtration, the solvent was evaporated and the crude was purified by silica gel chromatography (EtOAc/Heptane = 1:12) to give **18** (1.828 g, 98 %) as a yellow solid. ^{1}H NMR (400 MHz, Chloroform-*d*): δ 3.79 (t, *J* = 4.77 Hz, 1H), 2.48 – 2.33 (m, 2H), 2.28 – 2.16 (m, 3H), 2.04 – 1.86 (m, 2H), 1.71 – 1.50 (m, 3H), 1.26 – 1.15 (m, 1H), 1.09 (s, 3H), 0.89 (s, 9H), 0.04 (s, 6H). ^{13}C NMR (101 MHz, Chloroform-*d*): δ 213.3, 79.9, 43.6, 42.5, 36.9, 32.5, 32.3, 28.4, 25.8, 20.4, 18.1, -4.4, -4.8.

(5*R*)-2-Bromo-8-hydroxy-5,8-dimethyl-5,6,7,8,9,10-hexahydro-5,9-methanobenzo[8] annulen-11-one (20). Compound **20** was prepared in the same manner as **5**. Starting from 6-bromo-1-methyl-3,4-dihydronaphthalen-2(1H)-one (2 g, 8.36 mmol, 1 equiv) and *R*-(-)-α-methylbenzylamine (1.113 g, 9.19 mmol, 1.1 equiv), the intermediate **20** was obtained by silica gel chromatography (EtOAc/Heptane = 1:2) to yield compound **20** (1.7 g, 65%) as a brown solid. ^{1}H NMR (400 MHz, DMSO-d_6): δ 7.41 – 7.36 (m, 1H), 7.35 – 7.33 (m, 1H), 7.22 – 7.18 (m, 1H), 3.19 (d, *J* = 4.32 Hz, 2H), 2.47 – 2.43 (m, 1H), 2.07 –

1.98 (m, 1H), 1.51 – 1.45 (m, 1H), 1.41 – 1.34 (m, 1H), 1.31 (s, 3H), 1.28 – 1.24 (m, 1H), 1.23 (s, 3H). ^{13}C NMR (101 MHz, DMSO-d_6): δ 212.7, 142.1, 137.2, 129.7, 129.6, 127.5, 119.5, 76.7, 56.3, 47.6, 33.7, 31.9, 27.4, 19.7.

(*S*)-7-Bromo-4a-methyl-4,4a,9,10-tetrahydrophenanthren-2(3*H*)-one (21). Compound **21** was prepared in the same manner as **6**. Starting from **20** (1.7 g, 5.50 mmol, 1 equiv), compound **21** was obtained by silica gel chromatography (EtOAc/Heptane = 1:5) to yield compound **21** (560 mg, 35%) as a yellow solid. ^{1}H NMR (400 MHz, Chloroform-*d*): δ 7.39 – 7.32 (m, 1H), 7.25 – 7.24 (m, 1H), 7.18 – 7.14 (m, 1H), 5.91 – 5.89 (m, 1H), 3.02 – 2.95 (m, 1H), 2.92 – 2.82 (m, 1H), 2.76 – 2.63 (m, 2H), 2.57 – 2.48 (m, 2H), 2.37 – 2.31 (m, 1H), 2.09 – 1.99 (m, 1H), 1.55 (s, 3H). ^{13}C NMR (101 MHz, DMSO-d_6): δ 197.5, 168.6, 143.3, 137.5, 130.7, 129.5, 128.7, 123.7, 118.8, 38.7, 36.0, 34.3, 30.1, 29.7, 27.0.

(2*S*,4a*S*)-7-Bromo-4a-methyl-1,2,3,4,4a,9-hexahydrophenanthren-2-ol (22). To the solution of **21** (100 mg, 0.34 mmol, 1 equiv) in EtOAc (5 mL) and Ac_2O (0.66 mL) was added 4 mL $HClO_4$ in EtOAc (stock solution: 0.2 mL $HClO_4$ in 250 mL EtOAc) dropwise. The resulting mixture was stirred at room temperature for 10 min before diluted with saturated $NaHCO_3$ solution repeatedly. The organic phase was then evaporated and dissolved in ethanol (2 mL) and treated with $NaBH_4$ (104 mg, 2.73 mmol, 8 equiv) at 0° C for 6 h before quenched with HOAc (0.16 mL). The solvent was evaporated and then diluted with water (10 mL) followed by extraction with EtOAc (3 × 10 mL). The combined organic phase was dried over Na_2SO_4 and evaporated. The crude residue was purified by silica gel chromatography (Heptane/EtOAc = 3:1) to yield **22** (20 mg, 19 %) as a white solid. ^{1}H NMR (400 MHz, DMSO-d_6): δ 7.36 – 7.31 (m, 2H), 7.28 – 7.25 (m, 1H), 5.55 – 5.51 (m, 1H), 4.72 (d, *J* = 4.62 Hz, 1H), 3.35 – 3.32 (m, 1H), 2.37 – 2.30 (m, 1H), 2.27 – 2.22 (m, 1H), 2.18 – 2.12 (m, 1H), 1.82 – 1.77 (m, 1H), 1.66 – 1.55 (m, 1H), 1.40 – 1.30 (m, 1H), 1.28 (s, 3H), 1.27 – 1.21 (m, 1H). ^{13}C NMR (101 MHz, DMSO-d_6): δ 143.9, 138.8, 135.5, 130.7, 129.5, 129.0, 118.9, 118.1, 69.9, 42.3, 38.1, 37.2, 32.3, 29.3, 26.9.

HEK cell culture, mutagenesis, and transient transfections. HEK293 cells were grown, passaged and transiently transfected as described previously.[38] Briefly, cells were surface-grown and maintained at 37˚C in 10 cm (diameter) culture dishes in DMEM supplemented with 10% v/v fetal calf serum, 100 U/mL penicillin-G and 100 μg/mL streptomycin in a humidified (95% air/5% CO_2) incubator. When passaging, 0.05% w/v trypsin-EDTA was used to dislodge cells from the growth substratum.

The $\alpha1^{Q241L}$ mutation was introduced into murine wild-type α1 using standard PCR, gel electrophoresis, gel purification, DNA ligation, bacterial transformation, and DNA purification techniques and confirmed in full-length DNA sequencing (forward primer: CCtAGTCTCCTTCTGGCTCAACAGAG, reverse primer: GAGAGAATAACTGTCATTATGCAC; both 5' → 3').

Murine wild-type $GABA_AR$ subunit DNA clones, α1, β3 and γ2L (referred to as γ2), and the α_1^{Q241L} mutation (all in the pRK5 vector) were used for transient transfections (all stock cDNA concentrations were 1 μg/μL). Prior to transfections, HEK cells were plated onto poly-L-lysine-coated 22 mm glass coverslips. Cells were transfected with α1 or α_1^{Q241L}, with β_3, γ_2 and eGFP cDNAs in a ratio of (1:1:3:1), using a standard calcium-phosphate precipitation protocol with 6 μg cDNA, 20 μl of 340 mM $CaCl_2$, and 24 μl of 2x HBS (50 mM HEPES, 280 mM NaCl, 2.8 mM Na_2HPO_4) per coverslip. Electrophysiology was performed 16 – 30 h after transfection.

Dissociated hippocampal neuronal cell cultures

Hippocampal cells were obtained from E18 Sprague-Dawley rat foetuses. Animals were sacrificed in accordance with the Animals (Scientific Procedures) Act 1986 and the hippocampi were isolated. Cells were enzymatically dissociated in 0.25%w/v trypsin, before mechanical trituration with flame-polished Pasteur pipettes, then resuspended in a plating medium containing Minimum Essential Medium (MEM), 5% v/v heat-inactivated horse serum, 5% v/v heat-inactivated foetal bovine serum, 10 units/mL penicillin-G, 10 µg/mL streptomycin, 2 mM glutamine and 20 mM glucose. Neurons were plated onto 18 mm diameter glass coverslips precoated with poly-L-orthnithine (Sigma). After three hours the plating medium was replaced with a maintenance medium comprising Neurobasal-A, 1% B-27™ supplement, penicillin-G 50 units/mL, streptomycin 50 µg/mL, 35 mM glucose and 2 mM glutamine. The maintenance medium was refreshed 7 days after plating for optimal neuronal growth.

Whole-cell voltage-clamp electrophysiology and drug solutions for recombinant $GABA_A$Rs. A Nikon Eclipse FN1 microscope with a 470 nm LED was used to identify transfected GFP fluorescing HEK cells prior to patching. Cells were perfused with Krebs solution containing (mM): 140 NaCl, 4.7 KCl, 1.2 $MgCl_2$, 2.52 $CaCl_2$, 11 Glucose and 5 HEPES (pH 7.4), whereas patch pipettes (3 – 4 MΩ) were filled with an intracellular solution containing (mM): 120 KCl, 1 $MgCl_2$, 11 EGTA, 30 KOH, 10 HEPES, 1 $CaCl_2$ and 2 ATP-K_2 (pH 7.2).

Cells were voltage-clamped at -40 mV using an Axopatch 200B amplifier (Molecular Devices, USA). Whole-cell $GABA_A$-currents were filtered at 5 kHz (-36 dB per octave), digitized at 50 kHz via a Digidata 1322A (Molecular Devices), and recorded to a PC using Clampex 10.7 (Molecular Devices). Series resistance was compensated at 70 %, and data with less than 20 % change in series resistance would be included in later analyses.

The non-steroidal compounds (**1a** – **c**, **2a** – **d**, **3$_{a/b}$**, **3a** – **h** and **4**) could not be dissolved directly in aqueous solution, so stocks had to be made in DMSO where the highest possible concentration achievable was 100 mM. We have previously established that DMSO must be diluted 1000-fold to ensure that no DMSO current response is observed; hence the maximum final concentration we could achieve was 100 μM for all compounds.

During experiments, drugs were applied to cells using a fast Y-tube delivery system. Non-steroidal drugs were always pre-applied before co-application with GABA.

Whole-cell voltage-clamp electrophysiology for neuronal GABA$_A$Rs.

GABA$_A$ receptor-mediated spontaneous IPSCs (sIPSCs) were recorded from untransfected hippocampal pyramidal cells between 12 and 16 days after plating using whole-cell voltage clamp. Thin-walled borosilicate patch electrodes were used (resistance: 3 – 5 MΩ) filled with an internal solution containing (in mM): 140 CsCl, 2 NaCl, 10 HEPES, 5 EGTA, 2 $MgCl_2$, 0.5 $CaCl_2$, 2 Na-ATP, 0.5 Na-GTP and 2 QX-314, pH 7.3. Neurons were externally perfused with a Krebs saline solution supplemented with 2 mM kynurenic acid (to block excitatory glutamatergic activity) at pH 7.3, and room temperature. Cells were selected for recording on the basis that they were pyramidal shaped and approximately equal in soma size. Cells were voltage-clamped at -60 mV with membrane currents filtered at 2 kHz with a Bessel filter (80 dB per decade) and digitised at 20 kHz via a Digidata 1440A (Molecular Devices). All data were detected and acquired through Clampex 10.7 (Molecular Devices). Recordings where series resistance changed by more than 25% were discarded and this was calculated by measuring the response of the membrane current to 50 ms, 10 mV hyperpolarising voltage steps applied at a frequency of 10 Hz. WinEDR ver 4.0.4was used to detect sIPSCs in the digitised recordings, while WinWCP ver 5.7.3

(Strathclyde University, J Dempster Software) was used to determine sIPSC amplitude, frequency and decay kinetics. GABA-mediated tonic currents were identified, in the presence of 2 mM kynurenic acid, by the application of the $GABA_A$ receptor antagonist, bicuculline (50 μM), monitored as an outward shift in the holding current.

Data and Statistical Analysis. Prism (Version 10, GraphPad Software, San Diego, USA) was used for statistical analysis, data fitting and graphing. Peak and steady-state currents were measured in relation to the baseline currents prior to drug application using ClampFit 10.7 (Molecular Devices).

Direct activation responses were calculated as a percentage of the drugs maximum response ('peak') in relation to a maximum GABA concentration (1 mM GABA; $GABA_{MAX}$).

Inhibition was calculated as a percentage of the drugs maximum response (either at peak or at steady-state) in relation to a 70 μM GABA concentration (~EC_{80}). To generate inhibition concentration-response curves data values were fitted to the following equation:

$$I/I_{max} = 1 - ([B]^n/(IC_{50}^n + [B]^n))$$

Where, I is the current response; [B], the concentration of the novel drug; n the slope coefficient; and IC_{50}, the drug concentration producing 50% inhibition of GABA current (inhibitory potency). In Table 1, the potency values are presented as pIC_{50} with 95% confidence intervals. The mean EC_{50} was transformed into a molar concentration according to:

$$pIC_{50} = -\mathrm{Log}IC_{50}.$$

Drug potentiation peak responses were calculated as a percentage of the response by 0.3 μM GABA (~EC_{10}). A concentration response curve was generated by fitting data points using the Hill equation:

$$I / I_{max} = (1 / (1 + (EC_{50} / [A])^n),$$

where the EC_{50} represents the concentration of the drug ([A]) inducing 50% of the maximal current evoked by a saturating concentration of the agonist, and n is the Hill coefficient.

Data points on histograms and graphs are represented as mean values ± standard error of the mean (SEM) error bars.

Data sets were compared using ANOVA with Tukey's multiple comparisons post-hoc tests where appropriate. Statistical labels on graphs are defined as: ns: not significant; *: $p < 0.05$, **: $p < 0.01$, and ****: $p < 0.0001$.

ASSOCIATED CONTENT

Supporting information. The Supporting Information is available free of charge.

Molecular formula strings (CSV)

The nonsteroidal ligands bound to nuclear receptors with Shape-Tanimoto score over 0.7 (Table S1), Characterization of compound **1a** by ROESY. (Figure S1), Characterization of compound **2b** by ROESY (Figure S2), Characterization of intermediate **17** by ROESY (Figure S3), Analytic HPLC traces of **3a** and **3b** (Figure S4), Characterization of compound **3a/b** by COSY (Figure S5), The ^{1}H NMR spectrum of **3a** and **3b** (Figure S6), Characterization of compound **3c** by COSY (Figure S7), Characterization of compound 3e by ROESY (Figure S8).

AUTHOR INFORMATION

Corresponding Authors

* Chemistry: Prof. Bente Frølund - Phone: +45 35336495; email: bfr@sund.ku.dk

* Pharmacology: Prof. Trevor G. Smart - Phone: 0044-207-3770; email: t.smart@ucl.ac.uk

ORCIDs

Bente Frølund: https://orcid.org/0000-0001-5476-6288

Trevor G Smart: https://orcid.org/0000-0002-9089-5375

Yue Xu: https://orcid.org/0000-0002-6410-4840

Martin Mortensen: https://orcid.org/0000-0002-5873-7107

Yongsong Tian: https://orcid.org/0000-0001-7084-9083

Francesco Bavo: https://orcid.org/0000-0003-3797-0900

Thomas Seidel: https://orcid.org/0000-0002-9815-6577

Present Addresses

For Y.X.: State Key Laboratory of Natural and Biomimetic Drugs, School of Pharmaceutical Sciences, Peking University, Beijing, 100191, China.

Author Contributions

Y.X. and T.S. designed the molecules and performed computational chemistry modellings. Y.X., Y.T., N.N.J. and F.B synthesized all compounds and carried out separation of regioisomers. M. M. and S.L. designed and performed receptor mutagenesis and the electrophysiology experiments. B.F. and T.G.S directed the study and obtained funding to support the work. The manuscript was written through contributions of all authors. All authors have given approval to the final version of the manuscript. ‡These authors contributed equally.

Funding Sources

Chinese Scholarship Council, UK-Medical Research Council, The Wellcome Trust, the Drug Research Academy and Simon Fougner Hartmanns Familiefond.

Notes

The authors declare no competing financial interest.

ACKNOWLEDGMENT

The authors gratefully acknowledge Prof. Thierry Langer and Dr. Oliver Wieder's help and support for this project.

ABBREVIATIONS

GABA, γ-aminobutyric acid; $GABA_A$Rs, $GABA_A$ receptors; CNS, central nervous system; NASs, neuroactive steroids; PS, pregnenolone sulfate; PAM, positive allosteric modulator; NAMs, negative allosteric modulators; DHEAS, dehydroepiandrosterone sulfate; PBC, primary biliary cholangitis; HE, hepatic encephalopathy; ROCS, Rapid Overlay of Chemical Structures; HWE, Horner–Wadsworth–Emmons; MVK, methyl vinyl ketone; PDB, Protein Data Bank; TBDMS, tert-Butyldimethylsilyl; ROESY, Rotating frame Overhauser Effect Spectroscopy; COSY, Correlation Spectroscopy; TLC, Thin-layer chromatography; HPLC, High-performance liquid chromatography; UPLC, Ultra-high performance liquid-chromatography.

REFERENCES

(1) Sigel, E.; Steinmann, M. E. Structure, function, and modulation of GABA(A) receptors. *J. Biol. Chem.* **2012**, *287* (48), 40224-40231.
(2) Braat, S.; Kooy, R. F. The GABAA receptor as a therapeutic target for neurodevelopmental disorders. *Neuron.* **2015**, *86* (5), 1119-1130.
(3) Belelli, D.; Lambert, J. J. Neurosteroids: endogenous regulators of the GABA(A) receptor. *Nat. Rev. Neurosci.* **2005**, *6* (7), 565-575.

(4) Laverty, D. T., P.; Field, M.; Andersen, O. J.; Gold, M. G.; Biggin, P. C.; Gielen, M.; Smart, T. G. Crystal structures of a GABAA-receptor chimera reveal new endogenous neurosteroid-binding sites. *Nat. Struct. Mol. Biol.* **2017**, *24* (11), 977-985.
(5) Miller, P. S.; Scott, S.; Masiulis, S.; De Colibus, L.; Pardon, E.; Steyaert, J.; Aricescu, A. R. Structural basis for GABA(A) receptor potentiation by neurosteroids. *Nat. Struct. Mol. Biol.* **2017**, *24* (11), 986-992.
(6) Chen, Z. W.; Bracamontes, J. R.; Budelier, M. M.; Germann, A. L.; Shin, D. J.; Kathiresan, K.; Qian, M. X.; Manion, B.; Cheng, W. W. L.; Reichert, D. E.; et al. Multiple functional neurosteroid binding sites on GABAA receptors. *PLoS Biol.* **2019**, *17* (3), e3000157.
(7) Legesse, D. H. F., C.; Teng, J.; Zhuang, Y.; Howard, R. J.; Noviello, C. M.; Lindahl, E.; Hibbs, R. E. Structural insights into opposing actions of neurosteroids on GABAA receptors. *Nat. Commun.* **2023**, *14* (1), 5091.
(8) Germann, A. L. P., S. R.; Tateiwa, H.; Sugasawa, Y.; Reichert, D. E.; Evers, A. S.; Steinbach, J. H.; Akk, G. Intrasubunit and intersubunit steroid binding sites independently and additively mediate α1β2γ2L GABAA receptor potentiation by the endogenous neurosteroid allopregnanolone. *Mol. Pharmacol.* **2021**, *100* (1), 19-31.
(9) Carl, P.; Hogskilde, S.; Lang-Jensen, T.; Bach, V.; Jacobsen, J.; Sorensen, M. B.; Gralls, M.; Widlund, L. Pharmacokinetics and pharmacodynamics of eltanolone (pregnanolone), a new steroid intravenous anaesthetic, in humans. *Acta Anaesthesiol. Scand.* **1994**, *38* (7), 734-741.
(10) Kanes, S.; Colquhoun, H.; Gunduz-Bruce, H.; Raines, S.; Arnold, R.; Schacterle, A.; Doherty, J.; Epperson, C. N.; Deligiannidis, K. M.; Riesenberg, R.; et al. Brexanolone (SAGE-547 injection) in post-partum depression: a randomised controlled trial. *Lancet* **2017**, *390* (10093), 480-489.
(11) Powell, J. G.; Garland, S.; Preston, K.; Piszczatoski, C. Brexanolone (Zulresso): Finally, an FDA-Approved Treatment for Postpartum Depression. *Ann. Pharmacother.* **2020**, *54* (2), 157-163.
(12) Clayton, A. H. L., R.; Parikh, S. V.; Iosifescu, D. V.; Jung, J.; Kotecha, M.; Forrestal, F.; Jonas, J.; Kanes, S. J.; Doherty, J. Zuranolone for the Treatment of Adults With Major Depressive Disorder: A Randomized, Placebo - Controlled Phase 3 Trial. *Am. J. Psychiatry.* **2023**, appi. ajp. 20220459.
(13) Deligiannidis, K. M.; Meltzer-Brody, S.; Gunduz-Bruce, H.; Doherty, J.; Jonas, J.; Li, S.; Sankoh, A. J.; Silber, C.; Campbell, A. D.; Werneburg, B.; et al. Effect of Zuranolone vs Placebo in Postpartum Depression: A Randomized Clinical Trial. *JAMA Psychiatry.* **2021**, *78* (9), 951-959.
(14) den Hartigh, A. B.; Loomis, W. P.; Anderson, M. J.; Frolund, B.; Fink, S. L. Muscimol inhibits plasma membrane rupture and ninjurin-1 oligomerization during pyroptosis. *Commun Biol* **2023**, *6* (1), 1010. DOI: 10.1038/s42003-023-05354-4 From NLM Publisher.
(15) Majewska, M. D. D., S.; Spivak, C. E.; London, E. D. The neurosteroid dehydroepiandrosterone sulfate is an allosteric antagonist of the GABAA receptor. *Brain Res.* **1990**, *526* (1), 143-146.
(16) Wang, M. H., Y.; Eisenman, L. N.; Fields, C.; Zeng, C.-M.; Mathews, J.; Benz, A.; Fu, T.; Zorumski, E.; Steinbach, J. H. 3β-hydroxypregnane steroids are pregnenolone sulfate-like GABAA receptor antagonists. *J. Neurosci.* **2002**, *22* (9), 3366-3375.
(17) Lamb, Y. N. Ganaxolone: First Approval. *Drugs* **2022**, *82* (8), 933-940. DOI: 10.1007/s40265-022-01724-0 From NLM Medline.
(18) Blanco, M. J.; La, D.; Coughlin, Q.; Newman, C. A.; Griffin, A. M.; Harrison, B. L.; Salituro, F. G. Breakthroughs in neuroactive steroid drug discovery. *Bioorg Med Chem Lett* **2018**, *28* (2), 61-70. DOI: 10.1016/j.bmcl.2017.11.043 From NLM Medline.

(19) Martinez Botella, G. S., F. G.; Harrison, B. L.; Beresis, R. T.; Bai, Z.; Shen, K.; Belfort, G. M.; Loya, C. M.; Ackley, M. A.; Grossman, S. J. J. J. o. M. C. Neuroactive steroids. 1. Positive allosteric modulators of the (γ-aminobutyric acid) A receptor: Structure–activity relationships of heterocyclic substitution at C-21. *J. Med. Chem.* **2015**, *58* (8), 3500-3511.
(20) He, X. Y.; Wegiel, J.; Yang, S. Y. Intracellular oxidation of allopregnanolone by human brain type 10 17beta-hydroxysteroid dehydrogenase. *Brain Res.* **2005**, *1040* (1-2), 29-35.
(21) Vyklicky, V.; Krausova, B.; Cerny, J.; Balik, A.; Zapotocky, M.; Novotny, M.; Lichnerova, K.; Smejkalova, T.; Kaniakova, M.; Korinek, M.; et al. Block of NMDA receptor channels by endogenous neurosteroids: implications for the agonist induced conformational states of the channel vestibule. *Sci. Rep.* **2015**, *5* (1), 10935.
(22) Hawkins, P. C. S., A. G.; Nicholls, A. Comparison of shape-matching and docking as virtual screening tools. *J. Med. Chem.* **2007**, *50* (1), 74-82.
(23) Hawkins, P. C.; Skillman, A. G.; Warren, G. L.; Ellingson, B. A.; Stahl, M. T. Conformer generation with OMEGA: algorithm and validation using high quality structures from the Protein Databank and Cambridge Structural Database. *J. Chem. Inf. Model.* **2010**, *50* (4), 572-584.
(24) Park-Chung, M. M., A.; Purdy, R. H.; Gibbs, T. T.; Farb, D. H. Sulfated and unsulfated steroids modulate γ-aminobutyric acidA receptor function through distinct sites. *Brain Res.* **1999**, *830* (1), 72-87.
(25) Imamura, M. P., C. Modulation of GABA-gated chloride ion influx in the brain by dehydroepiandrosterone and its metabolites. *Biochem. Biophys. Res. Commun.* **1998**, *243* (3), 771-775.
(26) Mortensen, M.; Xu, Y.; Shehata, M. A.; Krall, J.; Ernst, M.; Frølund, B.; Smart, T. G. Pregnenolone sulphate analogues differentially modulate GABAA receptor closed/desensitised states. *Br. J. Pharmacol.* **2023**.
(27) Wadsworth, D. S. I., O.; Seus, E.; Ford Jr, J. J. T. J. o. O. C. The stereochemistry of the phosphonate modification of the Wittig reaction. *J. Org. Chem.* **1965**, *30* (3), 680-685.
(28) Morgan, B. P.; Swick, A. G.; Hargrove, D. M.; LaFlamme, J. A.; Moynihan, M. S.; Carroll, R. S.; Martin, K. A.; Lee, E.; Decosta, D.; Bordner, J. Discovery of potent, nonsteroidal, and highly selective glucocorticoid receptor antagonists. *J. Med. Chem.* **2002**, *45* (12), 2417-2424.
(29) Morgan, B. P. T., R. V.; Woodworth, G. F. New, Scalable Route for the Synthesis of a trans-Fused Hexahydro-1H-phenanthren-2-one from a Conjugated Tetrahydro-3H-phenanthren-2-one. *Synth. Commun.* **2003**, *33* (6), 915-920.
(30) Micheli, R. A. H., Z. G.; Cohen, N.; Parrish, D. R.; Portland, L. A.; Sciamanna, W.; Scott, M. A.; Wehrli, P. A. J. T. J. o. O. C. Total syntheses of optically active 19-nor steroids.(+)-Estr-4-ene-3, 17-dione and (+)-13. beta.-ethylgon-4-ene-3, 17-dione. *J. Org. Chem.* **1975**, *40* (6), 675-681.
(31) Hog, D. T. H., F. M.; Jiménez‐Osés, G.; Mayer, P.; Houk, K. N.; Trauner, D. J. C. A. E. J. Evolution of a Unified Strategy for Complex Sesterterpenoids: Progress toward Astellatol and the Total Synthesis of (−)‐Nitidasin. *Chem. Eur. J.* **2015**, *21* (39), 13646-13665.
(32) Zeng, C. Z., C.; Zhao, J.; Zhao, G. J. O. Divergent total syntheses of (−)-lycopladine D,(+)-fawcettidine, and (+)-lycoposerramine Q. *Org. Lett.* **2013**, *15* (22), 5846-5849.
(33) Gan, Y. S., T. A. Cholesterol surrogates incorporating a benzophenone as part of the sterol tetracycle. *J. Org. Chem.* **2006**, *71* (16), 5870-5875.
(34) Seljeset, S.; Bright, D. P.; Thomas, P.; Smart, T. G. Probing GABA(A) receptors with inhibitory neurosteroids. *Neuropharmacology* **2018**, *136* (Pt A), 23-36.

(35) Hosie, A. M. W., M. E.; Silva, H. M. A. da; Smart, T. G. Endogenous neurosteroids regulate GABAA receptors through two discrete transmembrane sites. *Nature* **2006**, *444* (7118), 486-489.
(36) Hosie, A. M. C., L.; Silva, H. M. A. da.; Smart, T. G. Conserved site for neurosteroid modulation of GABAA receptors. *Neuropharmacology* **2009**, *56* (1), 149-154.
(37) Sun, C.; Zhu, H.; Clark, S.; Gouaux, E. Cryo-EM structures reveal native GABA(A) receptor assemblies and pharmacology. *Nature* **2023**, *622* (7981), 195-201.
(38) Mortensen M, K. J., Kongstad KT, Brygger BM, Lenzi O, Francotte P, Sørensen TE, Nielsen B, Jensen AA, Smart TG, Frølund B. Developing new 4-PIOL and 4-PHP analogues for photoinactivation of γ-aminobutyric acid Type A receptors. *ACS Chem*. *Neurosci.* **2019**, *10* (11), 4669-4684.